



A Comprehensive Overview of the Genes and Functions Required for Lettuce Infection by the Hemibiotrophic Phytopathogen *Xanthomonas hortorum* pv. *vitians*

 Lucas Morinière,^a  Laurène Mirabel,^a  Erwan Gueguen,^b  Franck Bertolla^a

^aUniversité Lyon, Université Claude Bernard Lyon 1, CNRS, INRAE, VetAgro Sup, UMR Ecologie Microbienne, Villeurbanne, France


^bUniversité Lyon, Université Claude Bernard Lyon 1, INSA, CNRS, UMR Microbiologie, Adaptation, Pathogénie, Villeurbanne, France

ABSTRACT The successful infection of a host plant by a phytopathogenic bacterium depends on a finely tuned molecular cross talk between the two partners. Thanks to transposon insertion sequencing techniques (Tn-seq), whole genomes can now be assessed to determine which genes are important for the fitness of several plant-associated bacteria *in planta*. Despite its agricultural relevance, the dynamic molecular interaction established between the foliar hemibiotrophic phytopathogen *Xanthomonas hortorum* pv. *vitians* and its host, lettuce (*Lactuca sativa*), remains completely unknown. To decipher the genes and functions mobilized by the pathogen throughout the infection process, we conducted a Tn-seq experiment in lettuce leaves to mimic the selective pressure occurring during natural infection. This genome-wide screening identified 170 genes whose disruption caused serious fitness defects in lettuce. A thorough examination of these genes using comparative genomics and gene set enrichment analyses highlighted that several functions and pathways were highly critical for the pathogen's survival. Numerous genes involved in amino acid, nucleic acid, and exopolysaccharide biosynthesis were critical. The *xps* type II secretion system operon, a few TonB-dependent transporters involved in carbohydrate or siderophore scavenging, and multiple genes of the carbohydrate catabolism pathways were also critical, emphasizing the importance of nutrition systems in a nutrient-limited environment. Finally, several genes implied in camouflage from the plant immune system and resistance to immunity-induced oxidative stress were strongly involved in host colonization. As a whole, these results highlight some of the central metabolic pathways and cellular functions critical for *Xanthomonas* host adaptation and pathogenesis.

IMPORTANCE *Xanthomonas hortorum* was recently the subject of renewed interest, as several studies highlighted that its members were responsible for diseases in a wide range of plant species, including crops of agricultural relevance (e.g., tomato and carrot). Among *X. hortorum* variants, *X. hortorum* pv. *vitians* is a reemerging foliar hemibiotrophic phytopathogen responsible for severe outbreaks of bacterial leaf spot of lettuce all around the world. Despite recent findings, sustainable and practical means of disease control remain to be developed. Understanding the host-pathogen interaction from a molecular perspective is crucial to support these efforts. The genes and functions mobilized by *X. hortorum* pv. *vitians* during its interaction with lettuce had never been investigated. Our study sheds light on these processes by screening the whole pathogen genome for genes critical for its fitness during the infection process, using transposon insertion sequencing and comparative genomics.

KEYWORDS *Xanthomonas hortorum*, phytopathogen, lettuce, Tn-seq, comparative genomics

Editor Christopher W. Schadt, Oak Ridge National Laboratory

Ad Hoc Peer Reviewer  Steven Lindow, University of California, Berkeley

Copyright © 2022 Morinière et al. This is an open-access article distributed under the terms of the [Creative Commons Attribution 4.0 International license](https://creativecommons.org/licenses/by/4.0/).

Address correspondence to Franck Bertolla, franck.bertolla@univ-lyon1.fr.

The authors declare no conflict of interest.

Received 25 October 2021

Accepted 7 February 2022

Published 21 March 2022

Most Gram-negative bacterial plant pathogens behave as hemibiotrophs when interacting with their host plant (1). *Xanthomonas* species are indeed mostly considered hemibiotrophic pathogens that cause necrosis after a first asymptomatic phase (2–4). The infection process of a host plant by a nonvascular *Xanthomonas* is sequential: the pathogen displays different abilities in the cross talk with its host and ensures its own survival through nutrient acquisition systems and transformation of its micro-niche (5). *Xanthomonas* species initially start as epiphytes in the phyllosphere, an environment generally considered stressful and oligotrophic (6). There, in addition to deploying strategies to adhere to the leaf surface and survive abiotic stresses (7, 8), they rely on high-affinity TonB-dependent transporters (TBDTs) to take up simple sugars like sucrose and xylose (9, 10) or exploit more complex carbon sources (11). Biofilm formation at this stage participates in creating a safer and stable microenvironment for the population to develop (12).

The pathogen penetrates the leaves through natural openings (i.e., stomata, hydathodes, and wounds) and establishes itself within the apoplast to initiate its endophytic biotroph phase (5). It has to withstand the early basal responses triggered by the recognition of microbial-associated molecular patterns (MAMPs) by the plant pattern recognition receptors (PRRs) (13), feed on available nutrients, and synthesize compounds that are not directly available within its habitat. Polysaccharides such as cell-surface lipopolysaccharides (LPS) and the secreted exopolysaccharide (EPS) xanthan help to dampen the host immune response (14, 15). The type III secretion system (T3SS) also plays a major role in this phase, as it allows *Xanthomonas* species to disrupt the immune response signaling cascades and remodel the host metabolism to their own benefit through the intensive secretion of type III effectors (T3Es) (16, 17). Finally, the pathogen evolves toward a necrotrophic lifestyle: other cell death-inducing T3Es and the secretion of cell-wall-degrading enzymes (CWDEs) by the type II secretion system (T2SS) allow it to feed on leaked intracellular compounds and degraded cell components (1, 16).

Xanthomonas hortorum pv. *vitians* is a foliar pathogen of cultivated lettuce (*Lactuca sativa*); it causes a disease called bacterial leaf spot of lettuce (BLSL) (18), characterized by the progressive formation of small necrotic spots a few days after the pathogen has been inoculated. Then, these spots coalesce to form large necrotic patches that alter the quality and yield of the harvest without killing the entire plants (19, 20). BLSL has become a significant threat for lettuce producers over the past decades, and *X. hortorum* pv. *vitians* is considered a reemerging pathogen all around the world (18, 20–23). Nowadays, very little is known about the biology of this pathogen during the infection process, and the molecular bases sustaining the host-pathogen interaction remain mostly unelucidated (24).

To investigate the molecular biology and describe the essential genome of *X. hortorum* pv. *vitians* *in vitro*, a transposon insertion sequencing (Tn-seq) approach was recently developed for our model strain LM16734 (25). Tn-seq techniques rely on the generation of a saturated mutant library through large-scale transposon mutagenesis coupled with high-throughput next-generation sequencing and statistical analysis to estimate the essentiality and/or fitness contribution of each genetic feature in a selective environment (26). Tn-seq applications to bacteria of agricultural interest recently improved our understanding of the molecular cross talk between symbiotic or pathogenic bacteria and their host plants (27). For the plant-pathogenic species *Pantoea stewartii* subsp. *stewartii* (28), *Dickeya dadantii* (29), *Pseudomonas syringae* (30, 31), *Ralstonia solanacearum* (32), and *Agrobacterium tumefaciens* (33), Tn-seq provided an overall picture of the cellular functions and processes mobilized during plant infection and identified novel virulence factors.

We used our Tn-seq mutant library to screen for genes implied in lettuce colonization by *X. hortorum* pv. *vitians*. We applied a combination of comparative genomics, gene set enrichment analysis, and metabolic and cellular pathway mapping to draw biological sense from the list of genes defined as conditionally essential in lettuce. This approach successfully identified critical genetic features involved in amino acid and

nucleic acid biosynthesis, CWDE secretion by the T2SS, carbohydrate nutrition and iron uptake, cellular polysaccharide synthesis, and oxidative stress resistance systems.

RESULTS AND DISCUSSION

Validation of the Tn-seq experimental design and assessment of bottleneck effects. To investigate the fitness contribution of each genetic feature of *X. hortorum* pv. *vitians* LM16734 to growth in rich medium broth and during lettuce leaf infection, we used the previously developed and published Mariner-based Tn-seq mutant library (25). This library consists of at least 60,715 chromosomal mutants and 1,218 plasmidic mutants with transposon insertions at individual TA dinucleotide sites, out of a total of 85,314 chromosomal and 1,361 plasmidic TA sites within the *X. hortorum* pv. *vitians* LM16734 complete genome (5.23-Mb circular chromosome and 57-kb native plasmid pLM16734). The insertion densities in the library were ca. 71% and 89% on the chromosome and the plasmid, respectively.

First, the infection bottleneck effect arising from our inoculation procedure in young lettuce plants was estimated. The central paradigm behind Tn-seq experiments states that the mean read count per genetic feature is correlated with the corresponding mutant fitness in the tested selective environment (26). However, sampling bottleneck effects—which are stochastic events of loss of genetic diversity within a population when its size is drastically reduced (e.g., during host penetration and infection by a pathogen)—are known to blur data interpretation if not carefully considered in the experimental design (34, 35). Moreover, the selective DNA library preparation steps and random nature of mass sequencing can result in another type of bottleneck by reducing the genetic diversity within the extracted genomic library DNA (36). The number of generations experienced by the mutant library is also a critical parameter to be considered, as it directly impacts the fitness score calculated for each genetic feature (34, 37). Conceptually, a Tn-seq experiment consists of thousands of competition assays conducted simultaneously (34). Thus, variations in a mutant's abundance caused by selective pressure will be correlated with the number of generations experienced by the population.

A preliminary experiment was performed to estimate the number of bacterial cells spray-inoculated on lettuce leaves and the number of cells penetrating the leaves, as well as to monitor the population size over the course of infection. Approximately 2.5×10^4 CFU \cdot cm⁻² on average were deposited on the leaves during inoculation, and 5×10^3 CFU \cdot cm⁻² were measured inside the leaves after 24 h (Fig. 1a). Therefore, the theoretical successful infection ratio was 1:5, provided that no generation event occurred within this time interval. In reality, the founding population was likely to have been smaller than 5×10^3 CFU \cdot cm⁻², as a few generations probably occurred inside the leaves during the first 24 h. The generation time of *X. hortorum* pv. *vitians* is ca. 4.5 h in rich medium *in vitro* (data not shown). The total foliar surface for 30 plants was estimated to be approximately 6,000 cm², meaning that a total of 1.5×10^8 CFU were inoculated on the leaves and that 3×10^7 CFU were inside the leaves after 24 h. Regarding these estimations, a theoretical total mutant library coverage of 2,500 \times was inoculated, and a rough estimate of 50 \times to 500 \times maximum successfully invaded the plant tissue. Finally, the highest population level was achieved 10 days postinoculation (dpi), with an average of 5.6×10^6 internal CFU \cdot cm⁻² (Fig. 1a). Theoretically, 10 bacterial generation events occurred between 1 and 10 dpi, without considering mortality events. In other comparable *in planta* Tn-seq experiments, similar numbers of generations proved to be adequate for efficient and unbiased fitness score assessment (30, 31, 38).

Read mapping statistics showed that 22 to 26 million reads mapped to unique TA sites in the inoculum duplicates (T1 and T2), and 26 to 30 million in the lettuce infection duplicates (P1 and P2) (Table 1). The insertion densities were 69.9 and 71.0% on the chromosome and 88.5 and 87.9% on pLM16734 under the inoculum condition and 61.9 and 64.5% on the chromosome and 71.9 and 77.3% on pLM16734 under the *in planta* condition. Almost all library mutants were still present in the inoculum, and ca. 90% chromosomal and 80% plasmidic mutants were recovered in lettuce after 10 days. Moreover, Pearson correlation coefficients of read counts at unique TA sites between

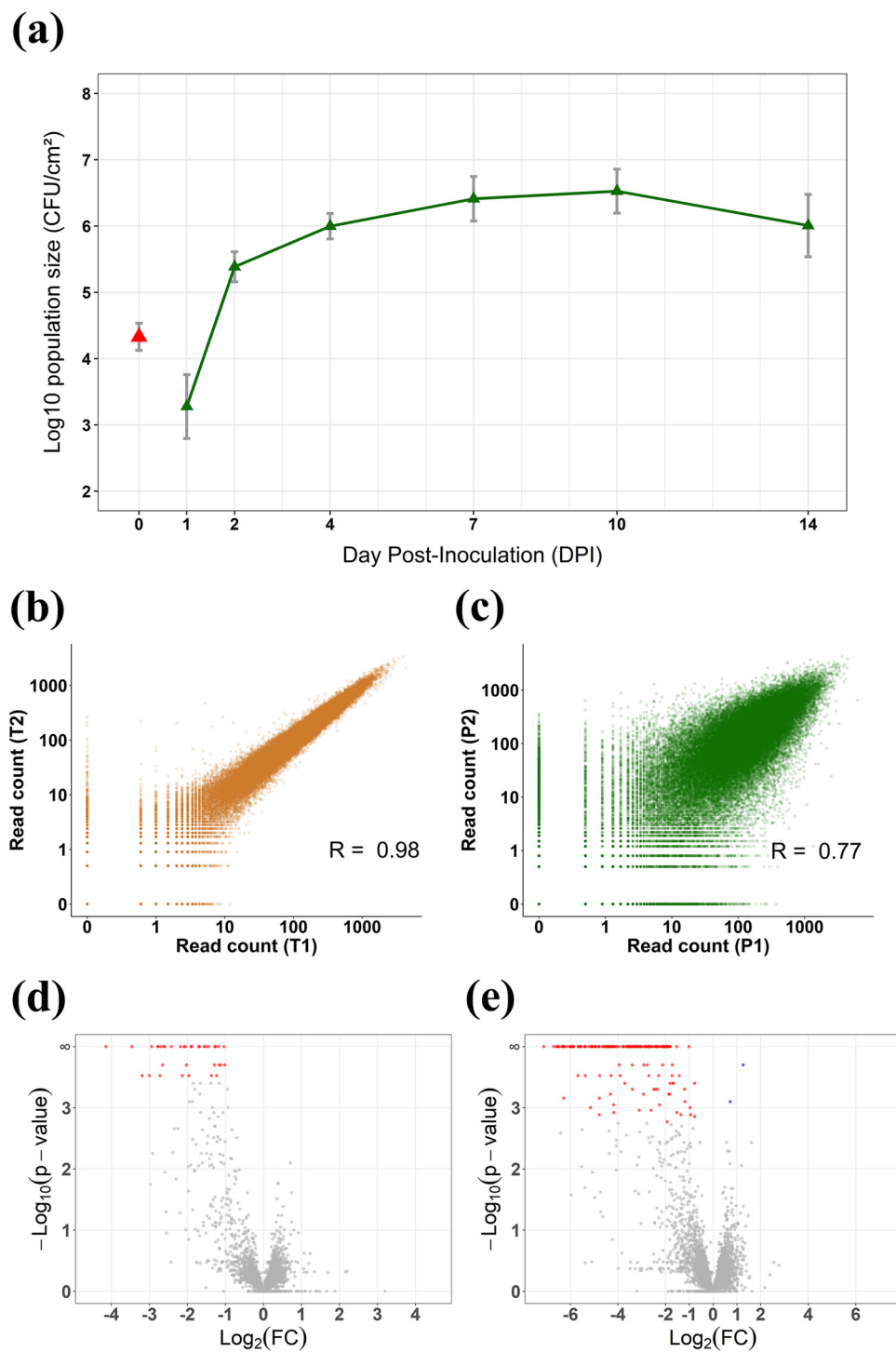


FIG 1 Validation of the experimental design and bottleneck assessment. (a) Evolution of the *X. hortorum* pv. *vitians* LM16734 population during lettuce infection, expressed as log₁₀-transformed CFU · cm⁻² of inoculated leaf. Red triangles, measured epiphytic populations following spray inoculation; green triangles, measured endophytic populations at each time point; gray bars, standard errors calculated on triplicates. (b and c) Read count correlation among Tn-seq duplicates for the *X. hortorum* pv. *vitians* LM16734 chromosome in (b) the inoculum and (c) lettuce leaves. (d and e) Volcano plots of the resampling results in (d) the inoculum versus the *in vitro* library condition and (e) lettuce leaves versus the inoculum condition. Plots represent the log₂ fold change of each genetic feature as a function of the negative log₁₀ of the resampling test *P* value. Genetic features that passed the FDR adjustment test (*q* value of ≤0.05) are indicated in red if they are conditionally essential and in blue if they provide a growth advantage. Nonsignificant genetic features are in gray.

TABLE 1 Transposon-insertion sequencing statistics before TTR normalization

Replicate	Sequencing yield	No. of Tn end-containing reads	Replicon	Read count (no. of unique TA sites)	No. of TA hits ^a	Insertion density ^b	Median read count over non-zero TA ^c
T1	25,830,465	22,029,814	Chromosome	21,916,438	59,675	69.9	100.9
			pLM16734	1,262,371	1,205	88.5	62.6
T2	39,102,386	26,462,594	Chromosome	26,330,348	60,579	71.0	99.6
			pLM16734	956,994	1,196	87.9	65.6
P1	30,091,641	26,195,853	Chromosome	26,067,795	52,850	61.9	99.9
			pLM16734	1,227,568	979	71.9	77.3
P2	34,333,964	30,135,609	Chromosome	29,982,890	55,013	64.5	93.8
			pLM16734	1,236,398	1,052	77.3	70.05

^aThe *X. hortorum* pv. *vitians* LM16734 genome contains 85,314 chromosomal TA sites and 1,361 plasmidic TA sites.

^bInsertion density reflects the percentage of TA sites with at least one read mapped over the total number of TA sites on the replicon.

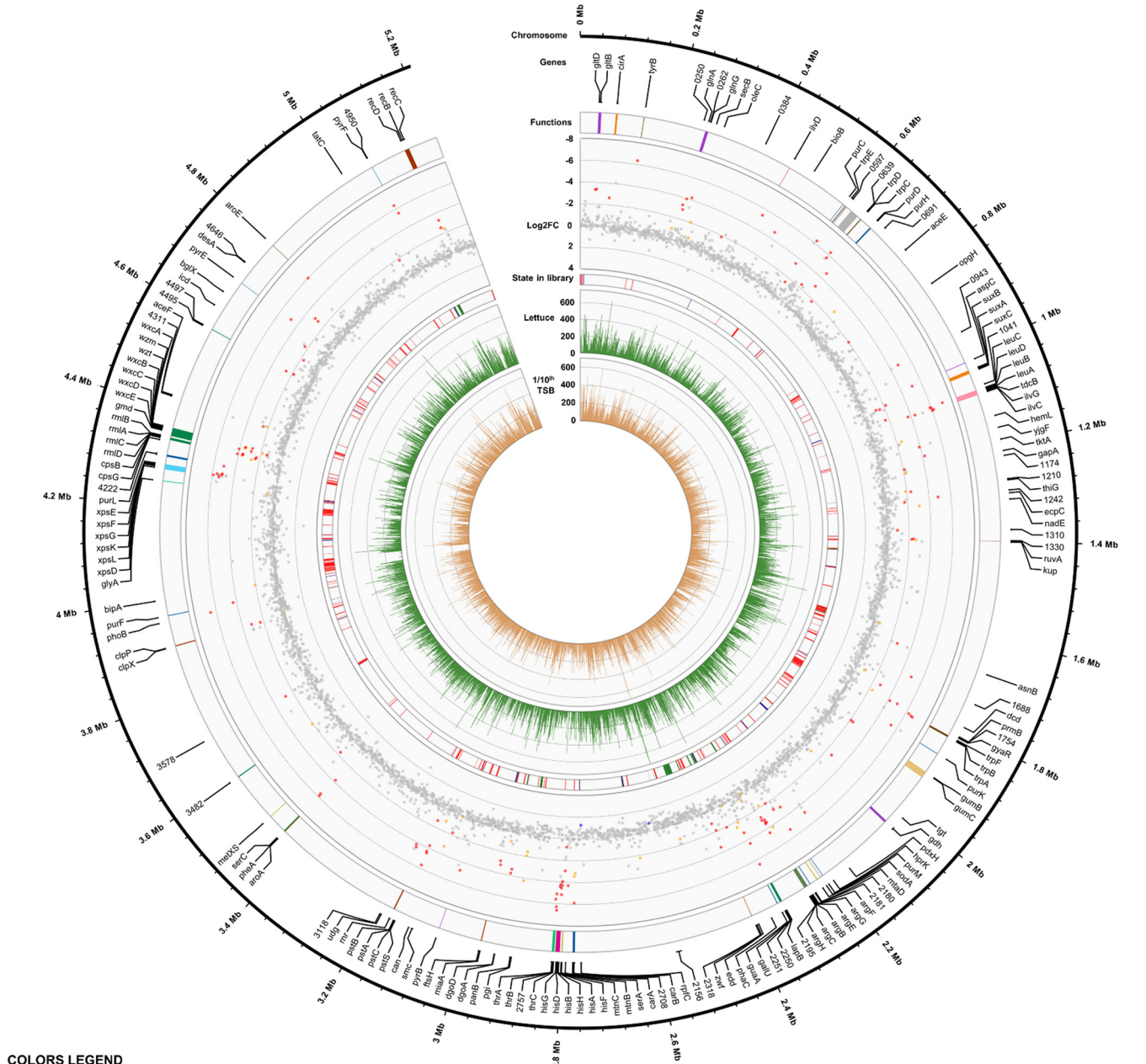
^cMean read count per TA site containing at least one read.

duplicates were 0.98 and 0.97 for the chromosome and plasmid pLM16734 under the inoculum condition, respectively, and 0.77 and 0.84 under the lettuce condition (Fig. 1b and 1c). These sequencing statistics confirmed that our experimental design bypassed the experimental bottleneck and that the technical bottleneck resulting from the DNA library preparation steps and sequencing was negligible.

Identification of 170 critical genes *in planta* and overrepresentation of anabolic processes. The resampling analyses conducted with TRANSIT identified 36 critical genes in 1/10th tryptic soy broth (TSB) medium (Fig. 1d) and 170 critical genes and two growth advantage genes in lettuce (Fig. 1e). The complete gene lists and associated resampling metrics are available in Tables S1 to S4 in the supplemental material. There was a partial overlap between the two critical gene sets, as 29 genes in lettuce leaf were already considered critical in 1/10th TSB. Additionally, we applied an extra filter by considering that mutants presenting a mean gene read count below 5 under the 1/10th TSB condition showed decreased fitness *in vitro*, and 8 more genes were classified as critical in 1/10th TSB. Examining the distribution of the critical genes in lettuce along the *X. hortorum* pv. *vitians* LM16734 chromosome revealed that a significant part seemed to be colocalized and organized in operons or gene clusters (Fig. 2).

To determine which biological processes, pathways, and functions were overrepresented in our lettuce critical gene set, Gene Ontology (GO) terms (39) and KEGG ortholog (KO) (40) identifiers were assigned to all *X. hortorum* pv. *vitians* LM16734 genes. The GO term enrichment analysis indicated that 43 GO terms were significantly enriched in our gene set (Table 2). Among the 35 biological process-related enriched GO terms, nucleotide, amino acid, polysaccharide, carbohydrate, nitrogen, and phosphorus metabolism-associated terms were most abundant. Overall, biosynthetic processes seemed to be more represented than degradation processes. For example, 67.7% of genes related to “Nucleobase biosynthetic process” (GO:0046112) versus 54.5% for “Nucleobase metabolic process” (GO:0009112) and 42.5% of genes associated with “Cellular amino acid biosynthetic process” (GO:0008652) versus 34.9% for “Cellular amino acid metabolic process” (GO:0006520) were identified. Interestingly, 5 out of 7 genes for “Phosphate ion transport” (GO:0006817) were also critical *in planta*.

The KEGG pathway analysis reached more precision in the identification of the most critical metabolic and cellular pathways *in planta* (Table 3). For instance, it highlighted that even though a total of 49.5% of the genes involved in the *de novo* biosynthesis of amino acids were critical in lettuce, the relative proportions of genes varied among the specific amino acid pathways. The most impacted biosynthetic pathways were those of arginine (92.3% of the genes), valine, leucine, and isoleucine (76.9%), and alanine, aspartate, and glutamate (64%) biosynthesis. The genes involved in these pathways were often colocalized, like the *leu* and *ilv* genes encoding part of leucine and isoleucine biosynthesis or the *arg* and *his* operons for arginine and histidine, respectively (Fig. 2). Similarly,



COLORS LEGEND

- Functions :**
- = Ala / Asp / Glu metabolism
 - = Gly / Ser / Thr biosynthesis
 - = Cys / Met metabolism
 - = Oxidative stress response
 - = Type II secretion system (*xps*)
 - = Val / Leu / Ile biosynthesis
 - = Arg biosynthesis
 - = Purine / Pyrimidine biosynthesis
 - = Xanthan biosynthesis (*gum* operon)
 - = Type III secretion system
 - = Phe / Tyr / Trp biosynthesis
 - = His biosynthesis
 - = LPS / O-antigen biosynthesis
 - = Carbohydrates scavenging systems

- Log₂FC :**
- = Critical in lettuce ($\log_2FC < 0$ & $q\text{-value} \leq 0.05$)
 - = Growth-advantage in lettuce ($\log_2FC > 0$ & $q\text{-value} \leq 0.05$)
 - = Critical in 1/10th TSB ($\log_2FC < 0$ & $q\text{-value} \leq 0.05$)
 - = Non-significant ($q\text{-value} \geq 0.05$)
- State in library :**
- = Essential
 - = Growth-defect
 - = Growth-advantage

FIG 2 Genome atlas of the critical genetic features required for lettuce infection by *X. hortorum* pv. *vitians* LM16734. From the inner to outer track are the mean read count over 1 kb in 1/10th TSB and in lettuce, the gene state in the *in vitro* library, as described in reference 24, the log₂ FC score in lettuce leaves compared to the inoculum, clustering of critical genes, pathways, functions and structural components in lettuce, gene names or locus tag identifiers, and chromosomal tracks.

TABLE 2 Significantly enriched Gene Ontology terms in the critical genes in the lettuce leaf subset

GO identifier	GO term	Total no. of genes ^a	No. of genes in subset ^b	Enrichment score ^c	<i>q</i> value ^d
Biological processes					
General processes					
GO:0006082	Organic acid metabolic process	298	64	2.686	0.0
GO:0016053	Organic acid biosynthetic process	167	49	2.188	0.0
GO:0044283	Small molecule biosynthetic process	226	56	1.965	0.0
GO:1901362	Organic cyclic compound biosynthetic process	233	39	1.696	0.006043
GO:0018130	Heterocycle biosynthetic process	223	37	1.7	0.008476
GO:0019438	Aromatic compound biosynthetic process	199	38	1.984	0.000196
GO:0046176	Aldonic acid catabolic process	4	3	5.8	0.033252
GO:0040007	Growth	90	14	2.543	0.035375
Nucleotide metabolism					
GO:0052803	Imidazole-containing compound metabolic process	12	6	5.887	0.011874
GO:0034654	Nucleobase-containing compound biosynthetic process	138	22	2.025	0.013182
GO:0055086	Nucleobase-containing small molecule metabolic process	124	26	1.901	0.015897
GO:0042435	Indole-containing compound biosynthetic process	6	5	5.292	0.017839
GO:0046112	Nucleobase biosynthetic process	9	6	4.451	0.022403
GO:1901293	Nucleoside phosphate biosynthetic process	73	20	2.205	0.000229
GO:0042430	Indole-containing compound metabolic process	11	7	7.289	0.000771
GO:0009112	Nucleobase metabolic process	11	6	4.42	0.03223
Amino acid metabolism					
GO:0006520	Cellular amino acid metabolic process	166	53	3.702	0.0
GO:0008652	Cellular amino acid biosynthetic process	94	40	2.453	0.0
GO:0009072	Aromatic amino acid family metabolic process	24	9	3.338	0.027736
GO:0000105	Histidine biosynthetic process	8	6	3.642	0.035375
Polysaccharide metabolism					
GO:0000271	Polysaccharide biosynthetic process	23	8	7.75	3.8e−05
GO:0033692	Cellular polysaccharide biosynthetic process	19	7	8.4	7.7e−05
GO:0044264	Cellular polysaccharide metabolic process	26	8	7.754	0.000214
GO:0005976	Polysaccharide metabolic process	35	9	6.524	0.00034
GO:0008653	Lipopolysaccharide metabolic process	12	6	5.546	0.003351
Carbohydrate metabolism					
GO:1901135	Carbohydrate derivative metabolic process	178	29	1.95	0.008547
GO:0046394	Carboxylic acid biosynthetic process	167	49	1.346	0.009947
GO:0006757	ATP generation from ADP	15	4	4.938	0.028161
Nitrogen and phosphate metabolism					
GO:0019637	Organophosphate metabolic process	147	25	2.12	0.008476
GO:0044106	Cellular amine metabolic process	17	7	5.333	0.008547
GO:0019627	Urea metabolic process	4	4	8.25	0.009169
GO:0071941	Nitrogen cycle metabolic process	6	4	7.754	0.027141
GO:0000050	Urea cycle	4	4	5.515	0.028161
GO:0006793	Phosphorus metabolic process	244	34	1.602	0.042509
GO:0006817	Phosphate ion transport	7	5	2.5	0.04326
Molecular functions					
GO:0016829	Lyase activity	93	21	3.246	0.000101
GO:0016614	Oxidoreductase activity, acting on CH-OH group of donors	49	11	3.6	0.002604
GO:0016879	Ligase activity, forming carbon-nitrogen bonds	42	12	1.907	0.008476

(Continued on next page)

TABLE 2 (Continued)

GO identifier	GO term	Total no. of genes ^a	No. of genes in subset ^b	Enrichment score ^c	q value ^d
GO:0048037	Cofactor binding	251	28	1.86	0.015897
GO:0005315	Inorganic phosphate transmembrane transporter activity	4	3	10.533	0.018301
GO:0016638	Oxidoreductase activity, acting on the CH-NH ₂ group of donors	8	4	8.333	0.024953
GO:0042802	Identical protein binding	144	19	1.661	0.033252
GO:0070279	Vitamin B6 binding	32	7	4.238	0.034385

^aTotal number of genes associated with the GO term in the *X. hortorum* pv. *vitians* LM16734 genome.

^bNumber of genes associated with the GO term in the subset of genes conditionally essential *in planta*.

^cThe simplified formula for the enrichment score (without pseudocounts) is $\log[(b/q)/(m/p)]$, where b is the number of genes with the GO term in the subset, q is the number of genes in the subset with a parent of the GO term, m is the total number of genes with the GO term in the genome, and p is the number of genes in the genome with a parent of the GO term. Thus, the enrichment score is the log-transformed ratio of the two relative abundances of genes with the GO term compared to those with a parent GO term (i) in the subset and (ii) in the complete genome. The calculation was derived from the Ontologizer method (114).

^dAdjusted P value using the Benjamini-Hochberg false-discovery rate (FDR) test. GO terms with a q value of <0.05 were considered significantly enriched.

19.6% of the carbon metabolism genes were critical, but the prevalent pathways were those of the 2-oxocarboxylic acid metabolism (57.1%), the pentose phosphate pathway (36%), the starch and sucrose metabolism (31.6%), and glycolysis/gluconeogenesis (29%). The genes related to the polysaccharide metabolism were mostly implied in O-antigen nucleotide sugar biosynthesis (56.3%). This analysis also pinpointed that 22.9% of the genes associated with the bacterial secretion systems were critical, which was not detected by the GO term enrichment analysis.

Overall, our results matched those of the other Tn-seq studies conducted on plant-pathogenic bacteria so far, in which many genes involved in the amino acid and nucleic acid metabolisms and in polysaccharide biosynthesis were critical *in planta* (28–30, 32). Moreover, random transposon mutant screening in other *Xanthomonas* species had already shown that mutating genes involved in these processes impaired growth and virulence *in planta* (41–44). For example, out of the 75 genes randomly screened as required for the virulence of *Xanthomonas campestris* pv. *campestris* in cabbage, 10 were involved in amino acid biosynthesis, 3 in *de novo* purine biosynthesis, 10 in lipopolysaccharide biosynthesis, and 3 in xanthan biosynthesis (41). This suggests that the central metabolic pathways required for plant colonization are equivalent across biological models and pathosystems, probably because plant-pathogenic bacteria face similar challenges in these selective environments: e.g., scarce nutrient or proteogenic amino acid availability.

Interestingly, no chemotaxis- or motility-related genes were screened as critical for the *in planta* lifestyle of *X. hortorum* pv. *vitians*, even though these features are usually considered important for pathogenicity and plant colonization (45). This could be explained by a combination of several factors. First, we hypothesized that during the spray-inoculation of our mutant library, some mutants may have been directly inoculated into the stomata and hydathodes. Thus, chemotaxis-driven motility was not required by these mutants to penetrate the leaves at the initial stages of plant infection. Second, motility might not be an indispensable feature for pathogenicity and *in planta* colonization by *Xanthomonas* species. A comparative genomic study of *Xanthomonas fuscans* subsp. *fuscans* suggested that the absence of motility could occur in field populations of several *Xanthomonas* species and that nonmotile variants would not undergo fitness defects in mixed populations, including flagellated strains (46). Furthermore, a new transcriptomic analysis of *X. campestris* pv. *campestris* conducted during cauliflower hydathode colonization revealed that the expression of most chemotaxis and motility genes was strongly repressed during the first days of infection (4). A similar observation was made during early rice infection by *Xanthomonas oryzae* pv. *oryzicola* (47). Such repression could even confer a stealth advantage to the bacterial population by reducing the production of microbial-associated molecular pattern (MAMP) molecules such as flagellar or pilus proteins (4, 46). Finally, chemotaxis and motility genes were not detected

TABLE 3 Critical KEGG pathways in *planta* (nonexhaustive)

Pathway code	KEGG pathway	No. of genes:		% of genes in pathway
		Critical ^a	Total ^b	
General and diverse pathways				
xhr01110	Biosynthesis of secondary metabolites	84	301	27.9
xhr01240	Biosynthesis of cofactors	19	128	14.8
xhr00910	Nitrogen metabolism	9	14	64.3
xhr03070	Bacterial secretion system	16	70	22.9
Amino acid metabolism				
xhr01230	Biosynthesis of amino acids	54	109	49.5
xhr00220	Arginine biosynthesis	12	13	92.3
xhr00290	Valine, leucine, and isoleucine biosynthesis	10	13	76.9
xhr00250	Alanine, aspartate, and glutamate metabolism	16	25	64
xhr00400	Phenylalanine, tyrosine, and tryptophan biosynthesis	11	26	42.3
xhr00260	Glycine, serine, and threonine metabolism	14	35	40
xhr00340	Histidine metabolism	6	18	33.3
xhr00270	Cysteine and methionine metabolism	11	37	29.7
Carbon compound metabolism				
xhr01200	Carbon metabolism	18	92	19.6
xhr01210	2-Oxocarboxylic acid metabolism	12	21	57.1
xhr00030	Pentose phosphate pathway	9	25	36
xhr00500	Starch and sucrose metabolism	12	38	31.6
xhr00010	Glycolysis/gluconeogenesis	9	31	29
xhr00052	Galactose metabolism	5	20	25
xhr00051	Fructose and mannose metabolism	5	21	23.8
Nucleobase metabolism				
xhr00240	Pyrimidine metabolism	7	25	28
xhr00230	Purine metabolism	11	54	20.4
Polysaccharide metabolism				
xhr00541	O-antigen nucleotide sugar biosynthesis	9	16	56.3

^aNumber of genes identified as conditionally essential in *planta* (q value of ≤ 0.05).

^bTotal number of genes in model pathway in the *X. hortorum*-specific KEGG pathway database.

in the *in planta* RB-Tn-seq study of *P. syringae*, neither in the epiphytic screening nor in the apoplastic one (30). The *in planta* transcriptome analysis of *Pseudomonas syringae* infecting *Arabidopsis thaliana* also demonstrated that these genes were downregulated during plant infection (48), consistent with the fact that plant-pathogenic *Xanthomonas* and *Pseudomonas* species share similar overall infection strategies.

Nutrient acquisition and assimilation as key features of the *in planta* lifestyle.

Numerous mutants of the carbohydrate metabolism were also strongly impaired in their fitness *in planta* (Tables 2 and 3). Interestingly, many genes of the central carbohydrate catabolism pathways—glycolysis and the pentose phosphate and Entner-Doudoroff pathways—were critical in lettuce, while none had been found indispensable on a glucose-rich medium (25). This time, most of the genes in these three pathways were conditionally essential either in lettuce or in 1/10th TSB medium (see Fig. S1 in the supplemental material), and so were some key genes of the starch and sucrose degradation and fructose and mannose degradation pathways (Table 3). Unfortunately, no information is available about the chemical composition of the lettuce leaf apoplast or surface. Sucrose and malate are generally the most abundant carbohydrates in the apoplast of eudicots (49–52). In any case, this apparent metabolic versatility most probably contributes to the pathogen's ability to adapt to the lettuce leaf environment, both outside and inside the leaf.

Consistent with numerous reports showing that *xps*-deficient *Xanthomonas* species mutants present reduced virulence *in planta* (41, 43, 44, 53), most of the *xps* T2SS mutants (XHV734_4180 to -4190) were positively screened as fitness deficient in our experiment (Fig. 3a). The *xps* genes that did not pass the significance threshold still displayed very low log₂ fold change (FC) values (Table S1), suggesting that, despite their

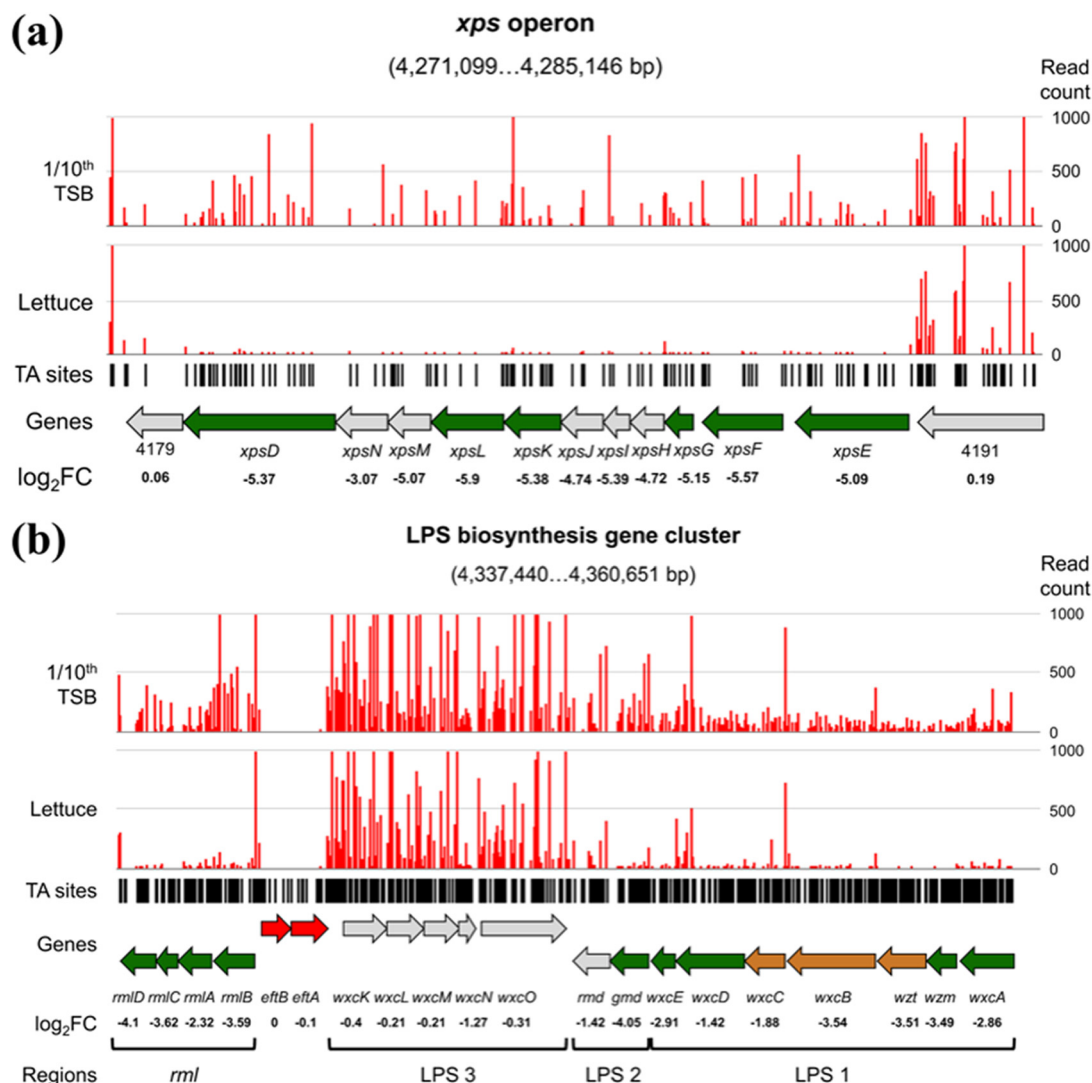


FIG 3 Schematic representation of (a) the critical genes in lettuce within the *xps* T2SS operon and (b) the LPS biosynthesis gene cluster of *X. hortorum* pv. *vitians* LM16734. Numbers in brackets indicate the width of the viewing window on the LM16734 genome. Green arrows, critical genes in lettuce; gold arrows, critical genes in 1/10th TSB; red arrows, essential genes in the *in vitro* library; gray arrows, nonsignificant genes. Gene names, log₂ FC values, and—for panel b—grouping in functional regions as described in reference 67 are displayed below. Black bars, localizations of TA sites; bar plots, read counts at each TA site under the control and experimental conditions. (Values of >1,000 are not displayed.)

rejection by the statistical test, they were also critical in lettuce. Like the *X. hortorum* pv. *gardneri* genome (54), the *X. hortorum* pv. *vitians* LM16734 genome contained a large repertoire of genes encoding CWDEs, including various pectinolytic, cellulolytic, and hemicellulolytic enzymes. These genes were not critical in our analysis, either because of their high functional redundancy or because of potential complementation in *trans* by neighboring cells. Once the cell wall polymers have been degraded by the type II-secreted CWDEs, breakdown products and simple oligosaccharides have to be internalized by the pathogen to be assimilated. This role has been mainly attributed to TonB-dependent transporters (TBDTs) in *Xanthomonas* species (10). These TBDTs are primarily known for their role in iron-siderophore uptake and are often associated with carbohydrate sensor or degrading genes in so-called carbohydrate scavenging systems or carbohydrate utilization with TBDT (CUT) loci (10, 11). They allow for the scavenging of carbohydrates with high affinity and are thought to play an important role in bacterial adaptation to oligotrophic environments, such as plants for phytopathogens (9).

Consequently, we searched for TBDT genes in our critical gene set and found three loci—XHV734_0066, -1016, and -1310—annotated as TonB-dependent receptors.

First, XHV734_1016 was located in the middle of a cluster of 3 critical genes (XHV734_1015 to -1017) (Fig. 2) which displayed a very strong homology and synteny with the *sux* CUT locus of *X. campestris* pv. *campestris*, responsible for sucrose-specific uptake and degradation (10). The *sux* gene cluster consists of *suxA* (XHV734_1016), coding for a sucrose TBDT that transports sucrose into the periplasm; *suxB* (XHV734_1015), coding for an intracellular amylosucrase that cleaves sucrose into glucose-1-P and fructose (55); *suxC* (XHV734_1017), coding for an inner membrane sucrose transporter; and *suxR* (XHV734_1018), coding for a LacI/GalR-family transcriptional repressor of sucrose import, which was logically not critical in our screening. The phosphohexose mutase encoded by *xanA* (XHV734_4228), which allows glucose-1-P to enter the glycolysis pathway, was also screened as critical. The conditional essentiality of this sucrose utilization locus in lettuce correlates with a previous study showing that sucrose was the primary carbon source of *X. campestris* pv. *campestris* in low-molecular-weight cabbage leaf extract during the first hours of incubation (56). Sucrose can also stimulate production of the diffusible signal factor (DSF) (57)—the *Xanthomonas* quorum-sensing signaling molecule that plays a major role in virulence regulation and survival *in planta* (58). Thus, sucrose may well be the preferential carbon source of *X. hortorum* pv. *vitians* during the early biotrophic phase of lettuce leaf invasion.

Second, XHV734_0066 was nearly identical to the *cirA* gene of *X. citri* subsp. *citri* 306, an oligoxyloside-specific TBDT involved in the uptake and utilization of xylan breakdown products (59). This *cirA* ortholog was adjacent to XHV734_0067, a xylose repressor-like transcriptional regulator strongly homologous to *xylR*, which regulates xylan degradation (9). Xylan from the cell wall hemicelluloses is mainly degraded into xylooligosaccharides by β -1,4-endoxylanases (60). *cirA* has been hypothesized to transport methylglucuronoxylotriose (MeGX₃)—a tetrasaccharide intermediate of xylan degradation—into the periplasm, where it can be converted into xylotriose by a membrane-bound α -glucuronidase (59). There, xylotriose can be either broken down into D-xylose or directly transported to the cytoplasm. Once in the cytoplasm, D-xylose is converted into D-xylulose-5-P by XylA1, XylA2, and XylB (XHV734_2842, -4908, and -2843), processed by the pentose phosphate pathway (PPP), and finally assimilated (9). Intriguingly, the *tktA* gene encoding the transketolase of the PPP that catalyzes the conversion of D-xylulose-5-P into glyceraldehyde-3-P was critical for fitness, but the *xylA* and *xylB* genes were not. Therefore, their function could be redundant or performed by other enzymes. Xylan exploitation is important for *Xanthomonas* nutrition during the early phyllosphere colonization stage (9), but xylan could also be an important nutrient during the late necrotrophic phase when host cells are actively degraded.

Finally, XHV734_1310 carries a homolog of the ferric enterobactin receptor *bfeA* of various *Xanthomonas* spp., which is flanked by two other similar copies (XHV734_1309 and -1312) and located upstream of the xanthoferrin siderophore biosynthesis and uptake gene cluster *xss* (XHV734_1298 to -1305) (61). The organization of these three *bfeA*-like genes upstream of *xss* is strikingly similar to what was observed in *X. citri* subsp. *citri* (62) and *X. oryzae* pv. *oryzae* (42). Wang et al. (42) named the genes *bfeA*, *bfeA2*, and *bfeA3* and reported that mutating *bfeA* alone ended up in a reduced-virulence phenotype *in planta*. Iron uptake using siderophores is indeed a well-known crucial feature of most bacterial phytopathogens necessary for successful host invasion (63). A recent proteomic analysis suggested that BfeA protein abundance could be directly correlated with virulence (64), which could partially explain why the gene is present in the form of three colocalized copies. However, further studies would have to elucidate why only one copy of *bfeA* is critical for fitness *in planta*.

Hiding from the plant immune system using cellular polysaccharides. The Tn-seq screening *in planta* highlighted a few critical genetic factors allowing *X. hortorum* pv. *vitians* to evade and counteract the lettuce immune response triggered by pathogen recognition during leaf invasion. The type III secretion system and its effectors are

probably the best-known factors used by *Xanthomonas* to disrupt the host immune response (17). However, the genes involved in the T3SS of *X. hortorum* pv. *vitians* LM16734 (XHV734_0611 to -0633) did not pass the statistical significance threshold in our Tn-seq analysis, even though almost all of them presented a moderate fitness defect (Table S1). Only *hrpF* (XHV734_0597) was considered critical; it encodes the translocon required for T3E translocation into host cells. In comparable *in planta* Tn-seq experiments conducted in *D. dadantii* (29) and *R. solanacearum* (32), genes of the T3SS apparatus were not critical either because of the variable efficiency of Tn-seq screens in detecting genes involved in production and secretion of “public goods” (65). On the other hand, the statistically significant screening of T3SS genes in *P. syringae* was attributed to low bacterial apoplastic densities that did not allow complementation in *trans* (30). Thus, it seems that the genetic diversity of the transposon mutants coexisting in lettuce apoplastic spaces was high enough to observe a partial complementation phenomenon of the T3SS roles.

Following the identification of the cellular polysaccharide metabolism as significantly enriched in the GO term enrichment analysis (Table 2), we searched for genes associated with these processes in our critical gene set. As a result, two genes of the *gum* gene cluster encoding the synthesis of the EPS xanthan and 19 genes involved in the biosynthesis and assembly of cell surface LPS, clustered in 3 distinct genomic regions, were identified (Fig. 2). We already discussed the lethal phenotypes observed in our Tn-seq library for the *gumE*, *gumI*, and *gumJ* mutants (25), but here only *gumB* (XHV734_1853) and *gumC* (XHV734_1854) were critical in lettuce leaves. These two genes, along with *gumE*, are responsible for polymerization of the lipid-linked pentasaccharide units and subsequent export of the final xanthan EPS out of the periplasm (66). Moreover, xanthan production by *gumB* and *gumC* mutants of *X. campestris* was completely abolished *in vivo* (67). Xanthan gum is required for full epiphytic survival and virulence in *Xanthomonas* species (12, 42, 68).

The remaining 19 genes associated with LPS biosynthesis and assembly emphasized the crucial importance of these surface components in the interaction with the host plant. Three main gene clusters were identified (Fig. 2), each encoding specific functions. The first region contained 4 genes: the conserved LPS assembly gene *lapB* (XHV734_2249) (69), a homolog of the *rfb303* gene of *X. citri* subsp. *citri* (XHV734_2250) putatively associated with biosynthesis of the LPS core (70), a putative sugar epimerase gene (XHV734_2251), and the *galU* gene (XHV734_2252), which is involved in O-antigen nucleotide sugar biosynthesis (66, 71). Another small gene cluster consisting of XHV734_4495 and -4497 was related to LPS biosynthesis. XHV734_4497 is an O-antigen ligase-like enzyme putatively involved in ligating the O-antigen and the lipid A core.

The principal LPS gene cluster corresponded to the major *rml/wxc* cluster of LPS biosynthesis (72). Tn-seq screening distinguished which parts of this cluster were critical and consequently which particular functions of the LPS biosynthesis process were required for growth in lettuce (Fig. 3b). First, the *rmlBACD* critical genes (XHV734_4231 to -4233) encode a set of enzymes that convert glucose-1-phosphate into the nucleotide sugar dTDP-L-rhamnose (73), which is the direct precursor of the rhamnose moieties of the *X. hortorum* pv. *vitians* LPS core and O-antigen (74). Then, the three functional regions of the LPS biosynthesis gene cluster (72) showed different results (Fig. 3b). The LPS 1 region located between *wxcA* (XHV734_4249) and *wxcE* (XHV734_4243) was entirely critical in lettuce and is responsible for the biosynthesis of the water-soluble O-antigen (72). Genes *wzt*, *wxB*, and *wxC* (XHV734_4247, -4246, and -4245) were also important for bacterial growth *in vitro*, suggesting that the formation of a functional O-antigen is necessary even in rich medium. Diverse *X. campestris* pv. *campestris* and *X. oryzae* pv. *oryzae* mutants defective in O-antigen biosynthesis showed reduced or abolished virulence *in planta* (41, 42). The *gmd* gene of LPS region 2 (XHV734_4242) was also critical in lettuce. This region is implied in biosynthesis of the core oligosaccharide of the LPS (72). Finally, none of the LPS 3 region genes, ranging from *wxcK* (XHV734_4236) to *wxcO* (XHV734_4240), was critical. Genes within this last segment probably encode accessory

synthesis and transfer of *N*-acetyl-3-amino hexose (72) and contribute to the side branching of the O-antigen (75). Mutating these genes resulted in the production of modified O-antigens in *X. campestris* pv. *campestris* (75).

Altogether, our findings indicate that certain genes directly implied in biosynthesis of the LPS core oligosaccharide and O-antigen are indispensable for successful bacterial invasion and survival inside lettuce leaves. Tn-seq also showed that some genes involved in biosynthesis of the LPS core and O-antigen were critical for *P. syringae* and *R. solanacearum* growth *in planta* (Table 4) (30, 32). Gram-negative bacterial LPS have a general protective role against stresses in diverse environments (76), including oxidative stress (70). They also participate in camouflaging pathogens from the host immune system, although they are also one of the major microbial-associated molecular patterns (MAMPs) recognized by host immunity receptors (77, 78). The long O-antigen of *Xylella fastidiosa* delays pathogen recognition and the basal immune response in grape (79). If a structurally intact LPS seems to be required for hiding from the lettuce immune system in *X. hortorum* pv. *vitiens*, modifications of the O-antigen side branching does not alter this protective role.

Diversity of resistance mechanisms to the immunity-triggered oxidative burst.

The rapid and localized accumulation of reactive oxygen species (ROS) inside the plant tissues following MAMP recognition by the plant PRRs is referred to as the oxidative burst (13). In general, protection against ROS-induced damage, which includes lipid peroxidation, enzyme inactivation, and nucleic acid degradation, can be achieved in three different ways: (i) prevention of ROS generation, (ii) detoxification of radicals, and (iii) repair of damaged elements (80). We found a set of 10 critical genes in lettuce that we hypothesized to actively participate in protecting the pathogen against the oxidative burst by detoxifying ROS and repairing damaged macromolecules (Fig. 2).

The Mn-superoxide dismutase-encoding gene *sodA* (XHV734_2154) was critical *in planta*. SodA plays a pivotal role in the virulence of several plant-pathogenic bacteria (81). The expression of this gene is induced within the first 3 h of infection in *X. campestris* pv. *campestris* and *D. dadantii* (82, 83), proving that it acts as a very early protection against the oxidative burst. Interestingly, *sodA* is not directly induced by ROS in *X. campestris* pv. *campestris*, but by redox cycling agents like plumbagin, a plant quinone with antimicrobial properties (84). Another gene, XHV734_2318, encodes an YgfZ-family folate-dependent protein that might also be involved in plumbagin resistance (85). On the other hand, *phaC* encodes a polymerase producing granules of poly(3-hydroxyalkanoate) (PHA), a polyester that can both serve as a form of carbon storage and can enhance resistance to cold and oxidative stresses in pseudomonads (81).

A variety of genes were implied in the recycling of misfolded proteins and damaged nucleic acids. The *clpX* (XHV734_3771), *clpP* (XHV734_3772), and *ftsH* (XHV734_2889) genes encode the ClpXP serine protease and an ATP-dependent Zn-metalloprotease, respectively. The ClpXP protease recycles misfolded proteins in the cytoplasm (86), and its inactivation in *X. campestris* pv. *campestris* through *clpX* or *clpP* mutations leads to pleiotropic effects, including increased stress sensitivity (87, 88). The *clpX* and *clpP* genes were also critical *in planta* in an *R. solanacearum* Tn-seq study (Table 4) (32). Moreover, oxidative stress induces the expression of *ftsH* in *Lactobacillus plantarum*, and Δ *ftsH* mutants are highly sensitive to various stresses (89). These two proteases are probably mobilized to buffer the damaging effects of the oxidative burst on the bacterial proteome.

Finally, the RNase R-encoding *rnr* gene (XHV734_3096) and the homologous genes of the recombination system *recBCD* (XHV734_5034, -5035, and -5033) were all critical in lettuce. They are probably involved in repairing the damage caused to nucleic acids by immunity-induced ROS production. RNase R is indeed required for the *trans*-translation pathway that directs deficient proteins and transcripts toward degradation while rescuing stalled ribosomes and is important for pathogenesis in many bacterial pathogens (90). This protein is overexpressed in *X. citri* subsp. *citri* during orange tree infection, supporting that it is important for *Xanthomonas* virulence (91). The RecBCD

TABLE 4 X. hortorum pv. *vitians* critical genes in lettuce with at least one homolog in other in *planta* Tn-seq/RB-Tn-seq studies conducted on plant-pathogenic bacteria

Locus	Gene	Product	Critical homologous gene(s) in:				Dickeya dadantii ^d
			<i>Pseudomonas syringae</i> ^a	<i>Ralstonia solanacearum</i> ^b	<i>Agrobacterium fabrum</i> ^c		
XHV734_0038	<i>gltD</i>	Glutamate synthase, 4Fe-4S protein, small subunit			ATU_RS17595		
XHV734_0039	<i>gltB</i>	Glutamate synthase, large subunit			ATU_RS17605		
XHV734_0130	<i>tyrB</i>	Tyrosine aminotransferase, tyrosine-repressible, PLP-dependent		RS_RS05000		Dda3937_01117	
XHV734_0259	<i>glnA</i>	Glutamine synthetase			ATU_RS02965	Dda3937_01116	
XHV734_0262		Two-component system sensor protein			ATU_RS07120		
XHV734_0263	<i>glnG</i>	Fused DNA-binding response regulator, sigma54 interaction protein			ATU_RS07125		
XHV734_0278	<i>secB</i>	Protein export chaperone		RS_RS01755			
XHV734_0458	<i>ilvD</i>	Dihydroxyacid dehydratase	P_syr_0469		ATU_RS09365		
					ATU_RS18520		
					ATU_RS14860		
XHV734_0506	<i>bioB</i>	Biotin synthase	P_syr_4687		ATU_RS11170		
XHV734_0595	<i>trpE</i>	Anthranilate synthase component 1	P_syr_4609	RS_RS14430	ATU_RS08260		
XHV734_0640	<i>trpD</i>	Anthranilate phosphoribosyltransferase	P_syr_4580		ATU_RS08265		
XHV734_0642	<i>trpC</i>	Indole-3-glycerol phosphate synthase			ATU_RS03175		
XHV734_0670	<i>purD</i>	Phosphoribosylglycinamide synthetase phosphoribosylamine-glycine ligase			ATU_RS13745	Dda3937_00244	
XHV734_0671	<i>purH</i>	Fused IMP cyclohydrolase; phosphoribosylaminoimidazolecarboxamide formyltransferase					
XHV734_0831	<i>opgH</i>	Glucans biosynthesis glucosyltransferase H	P_syr_0378	RS_RS14570	ATU_RS21970	Dda3937_03563	
XHV734_0943		Transcriptional regulator of N-acetylglucosamine utilization, LacI family			ATU_RS10725		
XHV734_0998	<i>aspC</i>	Putative aspartate aminotransferase					
XHV734_1041		Type I secretion outer membrane protein, TolC precursor					
XHV734_1046	<i>leuC</i>	3-Isopropylmalate isomerase subunit, dehydratase component	P_syr_1983		ATU_RS13195	Dda3937_00726	
XHV734_1047	<i>leuD</i>	3-Isopropylmalate isomerase subunit			ATU_RS13585	Dda3937_01352	
XHV734_1049	<i>leuB</i>	3-Isopropylmalate dehydrogenase	P_syr_1985		ATU_RS13590	Dda3937_04404	
XHV734_1050	<i>leuA</i>	2-Isopropylmalate synthase	P_syr_1257		ATU_RS11045	Dda3937_04301	
XHV734_1051	<i>tdcB</i>	L-Threonine dehydratase catabolic TdcB			ATU_RS05955		
XHV734_1053	<i>ilvG</i>	Acetolactate synthase isozyme 2 large subunit	P_syr_0846		ATU_RS09945		
XHV734_1054	<i>ilvC</i>	Ketol-acid reductoisomerase (NADP(+))	P_syr_0848		ATU_RS09860		
XHV734_1096	<i>hemL</i>	Glutamate-1-semialdehyde aminotransferase (aminomutase)			ATU_RS22545		
XHV734_1124	<i>yjgF</i>	Ketoacid-binding protein					
XHV734_1145	<i>tktA</i>	Transketolase 1, thiamin-binding			ATU_RS17355		
XHV734_1167	<i>gapA</i>	Glyceraldehyde-3-phosphate dehydrogenase A			ATU_RS17360		
XHV734_1174		Putative fructose-bisphosphate aldolase class 1			ATU_RS17375		
XHV734_1213	<i>thiG</i>	Thiamine biosynthesis ThiG complex subunit					
XHV734_1262	<i>nadE</i>	Glutamine-dependent NAD(+) synthetase					
XHV734_1330		Hypothetical protein					
XHV734_1332	<i>ruvA</i>	Component of RuvABC resolvase, regulatory subunit		RS_RS11780	ATU_RS17310		
XHV734_1688		Nicotinate-nucleotide adenyltransferase			ATU_RS17290		
XHV734_1761	<i>trpF</i>	N-(5'-Phosphoribosyl)anthranilate isomerase		RS_RS11005	ATU_RS00085		
XHV734_1763	<i>trpB</i>	Tryptophan synthase, beta subunit	P_syr_1663	RS_RS09970	ATU_RS00090		
XHV734_1765	<i>trpA</i>	Tryptophan synthase alpha chain	P_syr_0034	RS_RS09965	ATU_RS00095		
XHV734_1808	<i>purK</i>	N5-carboxyaminoimidazole ribonucleotide synthase	P_syr_0033	RS_RS09955	ATU_RS00095		
XHV734_1945	<i>tgt</i>	tRNA-guanine transglycosylase			ATU_RS17455	Dda3937_01683	
XHV734_1977	<i>gdh</i>	NAD-specific glutamate dehydrogenase		RS_RS13575	ATU_RS13460		

(Continued on next page)

TABLE 4 (Continued)

Critical homologous gene(s) in:						
Locus	Gene	Product	<i>Pseudomonas syringae</i> ^a	<i>Ralstonia solanacearum</i> ^b	<i>Agrobacterium fabrum</i> ^c	<i>Dickeya dadantii</i> ^d
XHV734_2148	<i>purM</i>	Phosphoribosylaminoimidazole synthetase			ATU_RS05630	Dda3937_02515
XHV734_2154	<i>sodA</i>	Superoxide dismutase, Mn			ATU_RS04315	
XHV734_2180		Dihydroorotase			ATU_RS06435	
XHV734_2250		UDP-N-acetylmuramyl pentapeptide phosphotransferase/UDP-N-acetylglucosamine-1-phosphate transferase			ATU_RS22585	
XHV734_2252	<i>galU</i>	UTP-glucose-1-phosphate uridylyltransferase	Psyr_2980	RS_RS08220	ATU_RS17570	
XHV734_2285	<i>phaC</i>	Poly(3-hydroxyalkanoate) polymerase subunit PhaC			ATU_RS02955	
XHV734_2316	<i>zwf</i>	Glucose-6-phosphate dehydrogenase				
XHV734_2707	<i>carB</i>	Carbamoyl-phosphate synthase large subunit				
XHV734_2709	<i>carA</i>	Carbamoyl phosphate synthetase small subunit, glutamine amidotransferase				
XHV734_2726	<i>serA</i>	D-3-Phosphoglycerate dehydrogenase	Psyr_4852		ATU_RS17200	Dda3937_01389
XHV734_2742	<i>hisF</i>	Imidazole glycerol phosphate synthase, catalytic subunit with HisH	Psyr_4894		ATU_RS00190	Dda3937_01390
XHV734_2743	<i>hisA</i>	N-(5'-Phospho-L-riboseyl-formimino)-5-amino-1-(5'-phosphoribosyl)-4-imidazolecarboxamide isomerase	Psyr_4894		ATU_RS00195	
XHV734_2744	<i>hisH</i>	Imidazole glycerol phosphate synthase, glutamine amidotransferase subunit with HisF	Psyr_4896		ATU_RS00200	
XHV734_2745	<i>hisB</i>	Fused histidinol-phosphatase; imidazoleglycerol-phosphate dehydratase	Psyr_4897		ATU_RS00210	
XHV734_2747	<i>hisD</i>	Bifunctional histidinol dehydrogenase and histidinol dehydrogenase	Psyr_4133		ATU_RS02645	
XHV734_2748	<i>hisG</i>	ATP phosphoribosyltransferase	Psyr_4134		ATU_RS03340	
XHV734_2829	<i>pgi</i>	Glucose-6-phosphate isomerase	Psyr_0826		ATU_RS01945	
XHV734_2887	<i>miaA</i>	Delta(2)-isopentenylpyrophosphate tRNA-adenosine transferase		RS_RS12855	ATU_RS09955	
XHV734_2989	<i>pyrB</i>	Aspartate carbamoyltransferase			ATU_RS06440	Dda3937_01284
XHV734_3113	<i>udg</i>	UDP-glucose 6-dehydrogenase			ATU_RS12570;	
					ATU_RS19395	
XHV734_3365	<i>aroA</i>	3-Phosphoshikimate 1-carboxyvinyltransferase		RS_RS04510		
XHV734_3366	<i>pheA</i>	Chorismate mutase/prephenate dehydratase			ATU_RS00480	
XHV734_3367	<i>serC</i>	3-Phosphoserine/phosphohydroxythreonine aminotransferase		RS_RS04490		
XHV734_3398	<i>metXS</i>	Homoserine O-succinyltransferase	Psyr_0474			
XHV734_3771	<i>clpX</i>	ATPase and specificity subunit of ClpX-ClpP	Psyr_1748	RS_RS08650		
XHV734_3772	<i>clpP</i>	Proteolytic subunit of ClpA-ClpP and ClpX-ClpP ATP-dependent serine protease		RS_RS08645		
XHV734_3851	<i>purF</i>	Amidophosphoribosyltransferase	Psyr_1668		ATU_RS05325	Dda3937_02099
XHV734_4155	<i>glyA</i>	Serine hydroxymethyltransferase	Psyr_4270	RS_RS03670		
XHV734_4196	<i>purL</i>	Phosphoribosylformyl-glycineamide synthetase	Psyr_1269			Dda3937_03379
XHV734_4228	<i>cpsG</i>	Phosphohexose mutase	Psyr_0219			
XHV734_4229	<i>cpsB</i>	Mannose-1-phosphate guanylyltransferase			ATU_RS15505	
XHV734_4230	<i>rmlD</i>	dTDP-4-dehydrothiamine reductase subunit, NAD(P)-binding, of dTDP-L-rhamnose synthase		RS_RS03435	ATU_RS21640	
XHV734_4231	<i>rmlC</i>	dTDP-4-deoxythiamine-3,5-epimerase				
XHV734_4232	<i>rmlA</i>	Glucose-1-phosphate thymidyltransferase			ATU_RS22530	
XHV734_4233	<i>rmlB</i>	dTDP-glucose 4,6-dehydratase		RS_RS03440	ATU_RS21635	
XHV734_4242	<i>gmd</i>	GDP-D-mannose dehydratase, NAD(P)-binding	Psyr_0915		ATU_RS21645	Dda3937_03924
XHV734_4247	<i>wzt</i>	ATP binding component of ABC-transporter	Psyr_0918			
XHV734_4248	<i>wzm</i>	Transport permease protein	Psyr_0917			

(Continued on next page)

TABLE 4 (Continued)

Locus	Gene	Product	Critical homologous gene(s) in:			
			<i>Pseudomonas syringae</i> ^a	<i>Ralstonia solanacearum</i> ^b	<i>Agrobacterium fabrum</i> ^c	<i>Dickeya dadantii</i> ^d
XHV734_4497		Lipid A core-O-antigen ligase-like enzyme		RS_RS11060		
XHV734_4610	<i>pyrE</i>	Orotate phosphoribosyltransferase			ATU_RS01925	Dda3937_03258
XHV734_4646		Flavodoxin reductases (ferredoxin-NADPH reductases) family 1			ATU_RS03585	
XHV734_4897	<i>tatC</i>	TatABCE protein translocation system subunit		RS_RS14730		

^aGenes required for *P. syringae* epiphytic and/or apoplasmic fitness in bean leaves according to Helmann et al. (30).

^bGenes required for *R. solanacearum* fitness in tomato plants according to Su et al. (32).

^cGenes required for *A. fabrum* fitness under at least one condition (i.e., tomato tumors, tomato roots, maize roots, or poplar tumors) according to Torres et al. (33).

^dGenes required for *D. dadantii* fitness in chicory leaves according to Royet et al. (29).

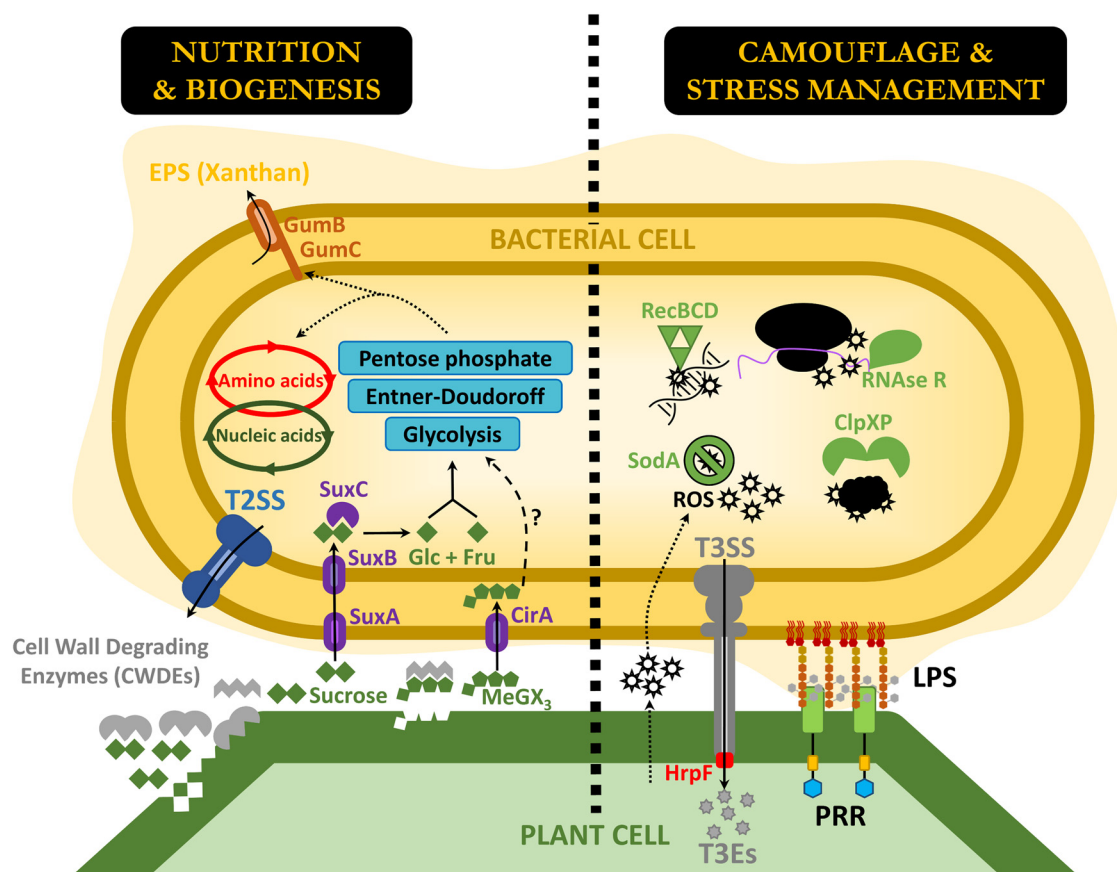


FIG 4 Schematic overview of the critical genes and processes required for lettuce infection by *X. hortorum* pv. *vitians* LM16734 as discussed in this work. Gray objects are known important virulence factors not screened as critical but discussed in the text. Abbreviations: EPS, exopolysaccharide; T2SS, type II secretion system; Glc, glucose; Fru, fructose; MeGX₃, methylglucuronoxylotriose; ROS, reactive oxygen species; T3SS, type III secretion system; T3Es, type III effectors; LPS, lipopolysaccharide; PRRs, pattern recognition receptors.

homologous recombination system has been proposed to be the predominant repair mechanism of oxidative stress-induced DNA damage (92–94), probably because it specifically repairs double-stranded breaks—the most deleterious DNA damage caused by oxidative agents (95). However, the *recC* mutant already showed a growth defect in the inoculum, and the *recBCD* genes all displayed low mean read count values *in vitro*. Intriguingly, RecA did not appear to play a role in oxidative stress resistance in *Xanthomonas* (96), which tends to be confirmed by its neutral status in our analysis.

Specific and common traits of the *in planta* lifestyle unveiled by the comparison with other plant-pathogenic bacteria. The present study presents a first overview of some of the molecular processes required for successful colonization and infection of lettuce leaves by the phytopathogenic bacterium *X. hortorum* pv. *vitians* (Fig. 4). Similar studies have been conducted on a handful of other plant-pathogenic bacteria *in planta* in the past 3 years, allowing us to compare the gene set we identified with those unveiled by other similar studies. We searched for homologs of the genes we identified in the data sets obtained for *D. dadantii* in chicory leaves (29), *P. syringae* in bean leaves (30), *R. solanacearum* in tomato roots (32), and *A. fabrum* under multiple conditions (tomato tumors and roots, maize roots, and poplar tumors) (33).

Eighty-three out of 170 critical genes of *X. hortorum* pv. *vitians* had at least one homolog in one of these other important plant-pathogenic bacterial genes *in planta* (Table 4). More precisely, 57 genes had homologs in *A. fabrum*, 33 in *P. syringae*, 21 in *R. solanacearum*, and 17 in *D. dadantii*, even though there was not a single gene found in all 5 studies. The importance of amino acid biosynthesis *in planta* was also true for *A. fabrum* and *P. syringae*, particularly in the Val/Leu/Ile, Ala/Asp/Glu, Phe/Tyr/Trp, Gly/

Ser/Thr, and His biosynthesis pathways, where most of the key genes were critical. Only the genes in the Phe/Tyr/Trp and Gly/Ser/Thr biosynthesis pathways were also critical in *R. solanacearum*, and only a few genes involved in the Val/Leu/Ile biosynthesis pathway were critical in *D. dadantii*. Most of the genes of the PPP and dDTP-L-rhamnose (a rhamnolipid and LPS component in several bacteria) biosynthesis pathways (97) were critical in both *X. hortorum* pv. *vitians* and *A. fabrum*. Finally, some key genes of the purine and pyrimidine biosynthesis pathways were important too in *A. fabrum* and *D. dadantii*. Overall, it appears that despite a few similarities, each of these 5 pathogens has specific nutritional requirements during its life *in planta*, probably because of the differential nutrient availability in the respective host plants.

Xanthomonas hortorum pv. *vitians* seems to be more dependent than the other pathogens on *de novo* amino acid biosynthesis. Besides the above-cited pathways, the 6 genes *argBCEFG* of the Arg biosynthesis pathway, *thrABC*, *gyaR*, and XHV734_4311 of the Gly/Ser/Thr biosynthesis pathway, and *mtaD* and *mtnBC* of the Cys/Met biosynthesis pathway were also important for fitness in lettuce leaves. Exogenous amino acid availability might therefore be scarcer in the lettuce apoplast than in the tomato, bean, or poplar leaf apoplasts. Mutagenesis of the T2SS was detrimental for *in planta* fitness of *X. hortorum* pv. *vitians*, but not for fitness of *R. solanacearum*, *P. syringae*, and *D. dadantii*. Yet, the T2SS is an important virulence factor for these three pathogens (29, 98, 99). Even though an *in trans* complementation effect could account for this phenomenon in the *D. dadantii* Tn-seq study (29), our results suggest that the T2SS may play an unexpectedly important role in the virulence of *X. hortorum* pv. *vitians*. A thorough comparison with other plant-pathogenic bacterial LPSs would be difficult because each bacterium has a specific set of genes involved in LPS biosynthesis (100–102). Yet, the accurate identification of the LPS biosynthesis genomic regions critical for *in planta* fitness of *X. hortorum* pv. *vitians* is also a new finding that strengthens our understanding of the role of this major surface component in *Xanthomonas* pathogenesis. Finally, several genes putatively implied in the degradation and repair of damaged nucleic acids or misfolded proteins (*recBCD*, *rnr*, *ftsH*, and XHV734_2318) were critical only in *X. hortorum* pv. *vitians*, while the *clpXP* protease was also important for *in planta* fitness of *P. syringae* and *R. solanacearum* (Table 4). However, different proteases were important *in planta* for the other pathogens: e.g., the *clpAP* protease for *A. fabrum* and *D. dadantii* (29, 33). Although the detrimental consequences of the plant defense mechanisms are relatively similar in all these pathosystems, it seems that each pathogen displays a specific response based on different genes.

More *in planta* Tn-seq studies will undoubtedly be conducted on other plant-pathogenic bacteria in the years to come. The next step will consist of extending the comparison conducted here to see if the gene sets important for *in planta* fitness of plant pathogens belonging to a same genus overlap. A comparison between pathogens conventionally classified as biotrophs or necrotrophs, soilborne or not, or between pathogens infecting a same plant species would also refine our understanding of the complex genetic requirements sustaining these host-pathogen interactions.

MATERIALS AND METHODS

Bacterial strains, growth conditions, and Tn-seq library generation. *Xanthomonas hortorum* pv. *vitians* LM16734 (=CFBP 8638) was originally isolated from a diseased leaf sample of oakleaf lettuce (*Lactuca sativa*) collected in the Rhône-Alpes region (France) in 2016 (18). The bacterium was routinely cultured on 1/10th tryptic soy agar (TSA) plates and in 1/10th tryptic soy broth (TSB) at 28°C. The procedure for generating the Tn-seq mutant library was described previously (25). Briefly, mating the recipient *X. hortorum* pv. *vitians* LM16734 strain with a donor *Escherichia coli* MFDpir/pSamEc strain containing a Himar1-C9 transposase gene yielded approximately 250,000 individual mutant colonies. They were recovered with 1/10th TSB, pooled, and stored in 30% (vol/vol) glycerol vials at –80°C. The resulting mutant library population was estimated to 10¹⁰ CFU · mL⁻¹.

Monitoring of the bacterial population *in planta*. The bacterial population was estimated over the course of the infection process in leaf lettuce cv. Météore for 14 days. Plants were cultivated and inoculated as described previously (18). The population size was enumerated 0, 1, 2, 4, 7, 10, and 14 days postinoculation (dpi). At each time point, three infected leaves from three different plants were randomly collected and treated as independent technical replicates. Except for the initial sampling at *t* = 0 dpi, aimed

at enumerating the inoculum deposited on the leaves, all other leaf samples were surface sterilized in a 70% ethanol bath for 20 s and rinsed in sterile deionized H₂O (dH₂O) to count only the bacteria that had penetrated the leaf tissue. In all cases, 4 disks of 3.14 cm² each were cut with a sterilized 1-cm-diameter punch on either side of the leaf midrib and pooled in 10 mL of sterile dH₂O. Leaf disks were crushed using a T25 IKA Ultra-turrax disperser (IKA, Staufen im Breisgau, Germany) at full speed. The resulting leaf homogenates were serially diluted and plated onto 1/10th TSA plates supplemented with cycloheximide at 50 μg · mL⁻¹ with an easySpiral automated plater (Interscience, Saint-Nom-la-Bretèche, France). The plates were incubated at 28°C for 4 days and enumerated with a Scan 1200 automatic colony counter (Interscience). Bacterial population sizes were expressed in CFU · cm⁻² of lettuce leaf.

Inoculation of lettuce with the transposon library. Two transposon library aliquots were thawed at 4°C overnight and inoculated in two flasks containing 100 mL of 1/10th TSB supplemented with kanamycin at 25 μg · mL⁻¹. The cultures were incubated overnight at 28°C under shaking at 120 rpm until they reached an optical density at 600 nm (OD₆₀₀) of 1.4. Then, they were centrifuged at 3,344 × *g* at 4°C for 20 min, and the cell pellets were washed by being resuspended in 25 mL of cold sterile dH₂O and repeating the centrifugation step. Each cleaned cell pellet was resuspended in sterile dH₂O and spectrophotometrically adjusted to obtain 400 mL of inoculum at an OD₆₀₀ of 0.2 supplemented with Tween 80 at 0.08% (vol/vol). Half of each inoculum was centrifuged, and the cell pellets were stored at -20°C for DNA extraction of the control condition. The remaining 200 mL of each inoculum was hand-sprayed on the leaves of 30 young lettuce cv. Météore plants per duplicate until runoff. All plants were immediately incubated in an Ineltec environmental chamber (Ineltec France, Vénissieux, France) at 25°C, with an 18-h photoperiod and 90% relative humidity (RH) for 48 h and then 70% RH for the rest of the experiment.

Recovery of bacterial cells from lettuce leaves. Diseased lettuce leaves were collected at *t* = 10 dpi, when small water-soaked leaf spot lesions were abundant but not coalescent, and duplicates were treated separately. Leaves were crushed in 500 mL of sterile dH₂O with a sterilized Moulinex Masterchef 58 electronic blender (SEB Moulinex G S M, Ecully, France) at middle speed for 2 to 3 min until <2-mm rough fragments were obtained. The resulting suspensions were sonicated in a sonication water bath 88155 (Fischer Bioblock Scientific, Illkirch, France) for 15 min to detach bacterial cells from leaf debris. To remove plant debris, the suspensions were successively filtered through 1-, 0.5-, 0.25-, and 0.05-mm-pore-diameter sieves, then twice through 20-μm-pore-diameter coffee filters, and finally vacuum filtered through 10-μm-pore ipPORE track-etched membrane filters (it4ip, Louvain-la-Neuve, Belgium). In the end, approximately 400 mL of filtered bacterial cell suspensions was recovered per duplicate and centrifuged at 10,647 × *g* for 20 min at 4°C, and the cell pellets were temporarily kept at -20°C.

DNA extraction and library preparation. Genomic DNA library extraction and preparation were conducted mostly as described previously (25), with technical variations. Briefly, the cell pellets were thawed, and genomic DNA was extracted using a Promega Wizard genomic DNA purification kit (Promega, Madison, WI, USA) and resuspended in 200 μL of Tris-EDTA (pH 7). Fifty micrograms of DNA per sample was digested with the Mmel restriction enzyme (New England Biolabs, Ipswich, MA, USA), and digestion products were purified. Samples were deposited on a 1% (wt/vol) agarose gel, and the 1.3- to 1.8-kb DNA fragments were cut out from the gel and retrieved using a QIAquick gel extraction kit (Qiagen, Hilden, Germany). Then, 300 to 500 ng of each sample was ligated to double-stranded bar-coded adapters with the T4 DNA ligase (New England Biolabs). The 20-bp genomic DNA regions flanking the transposon were amplified by 22 cycles of PCRs in 50-μL final volumes. The reaction mixtures contained 2 μL of ligated DNA matrix, 1 U of Q5 DNA polymerase (New England Biolabs), 1 × Q5 buffer, 0.2 mM deoxynucleoside triphosphates (dNTPs), and 0.4 μM of each TruSeq primers (Illumina, Inc., San Diego, USA). The PCR products were deposited on a 2% (wt/vol) agarose gel, and the 125-bp bands were extracted using a QIAquick gel extraction kit (Qiagen). Library DNA samples were sent to the I2BC-sequencing platform (I2BC, Gif-sur-Yvette, France) to be sequenced in the “High Output Single Read” 75-bp mode on a NextSeq 500 instrument (Illumina, Inc.).

Pretreatment of the sequencing read data. Raw reads were trimmed with CUTADAPT v1.15 (103) to filter those containing the Mariner inverted left repeat (i.e., ACAGTTGGATGATAAGTCCCCGGTCTT) and remove the adapter sequences. Trimmed data sets were mapped without mismatches to unique TA sites with a modified version of the TPP script from the TRANSIT software suite v2.0.2 (104) on the complete genome sequence of *X. hortorum* pv. *vitians* LM16734 available from the NCBI GenBank database under accession no. GCA_014338485.1. The script generating the prot_table file used by TRANSIT was modified to integrate noncoding RNA (ncRNA) features. *In vitro* library sequencing reads available in the NCBI SRA database under accession no. SRR12067051 and SRR12067052 were retrieved and combined with the newly generated sequencing reads in a single .wig file, and subjected to the “Trimmed Total Reads” (TTR) normalization method in TRANSIT v3.2.1.

Assessment of the contribution of each gene to fitness *in vitro* and *in planta*. The contribution of each genetic feature to bacterial fitness was determined both in 1/10th TSB (inoculum) and in lettuce by carrying out pairwise comparisons of (i) the inoculum condition with the previously generated *in vitro* library results (25) and (ii) the lettuce infection condition with the inoculum condition. Reads in the 5% N-terminal and 10% C-terminal portions of the genetic feature were discarded because they could lead to incorrect interpretations, and a LOESS (locally estimated scatterplot smoothing) correction for genome positional bias was applied. The “Resampling” method available in the TRANSIT v3.2.1 suite (105) was used to evaluate the fitness contribution and statistical significance of each genetic feature in the two comparisons, by (i) calculating the difference in the sum of read counts and log₂ fold change (FC) between the control and experimental conditions, (ii) calculating *P* values using variation of the non-parametric permutation test, and (iii) correcting the *P* values by performing a Benjamini-Hochberg false-discovery rate (FDR) test (106), which yields *q* values expressing the probabilities of false-positive results.

The genetic features with a q value of ≤ 0.05 were considered to present a significant fitness difference between the control and experimental conditions, and potential artifactual features were checked manually on the MicroScope platform (<https://mage.genoscope.cns.fr>) (107). Finally, the circular genome and data mapping were visualized with the R/Shiny application shinyCircos (108).

Gene annotation, Gene Ontology term enrichment, KEGG pathway mapping, and comparison with other Tn-seq or RB-Tnseq in planta experiments. A mixed annotation strategy was applied to assign Gene Ontology (GO) terms (39) to *X. hortorum* pv. *vitians* LM16734 genes. Protein sequences were extracted from the genome using the `cds_extractor` script from the `bac-genomic-scripts` suite (109). Terms were assigned using the web-based tool eggNOG-Mapper v2 (110) against the eggNOG v5.0 database (111) and InterproScan v5.0.0 (112), available on the Galaxy for Genome Annotation (GGA) server (<https://annotation.usegalaxy.eu/>) (113). Finally, a GO term enrichment analysis was conducted with the “Pathway Enrichment Analysis” method available in TRANSIT, based on the Ontologizer method (114). GO terms with an FDR-adjusted q value of ≤ 0.05 were considered to be significantly enriched in the gene subset. EC numbers, eggNOG orthologs, and Cluster of Orthologous Groups (COG) categories were also assigned with eggNOG-Mapper v2. The Kyoto Encyclopedia of Genes and Genomes (KEGG) (<https://www.kegg.jp/>) database was used to assign KEGG Orthology (KO) terms to genes with BlastKOALA v2.2 (40). KO terms were mapped to the *X. hortorum* reference pathways (*xhr*) with KEGG Mapper (115). Synteny and gene homology assessment were performed on the MicroScope platform following the guidelines of the MicroScope team annotation (107). Our data were compared with the genes identified as important for *in planta* fitness of *P. syringae* (30), *R. solanacearum* (32), *Agrobacterium fabrum* (33), and *D. dadantii* (29) by searching our *in planta* critical gene set for homologs of these genes using BLASTP. Genes with more than 50% coverage, 30% protein identity and an E value of $< 10^{-5}$ were considered homologs as described previously (25), and gene annotations and functions were consistently checked to prevent potential inconsistencies.

Data availability. The NCBI GenBank assembly accession number for the complete *X. hortorum* pv. *vitians* LM16734 genome is GCA_014338485.1. Transposon insertion sequencing raw reads have been deposited in the NCBI SRA database under accession no. [SRR14385278](https://www.ncbi.nlm.nih.gov/sra/SRR14385278) to [SRR14385281](https://www.ncbi.nlm.nih.gov/sra/SRR14385281). All data are associated with BioProject no. [PRJNA530964](https://www.ncbi.nlm.nih.gov/bioproject/PRJNA530964) and [PRJNA726806](https://www.ncbi.nlm.nih.gov/bioproject/PRJNA726806).

SUPPLEMENTAL MATERIAL

Supplemental material is available online only.

FIG S1, TIF file, 2.5 MB.

TABLE S1, XLSX file, 1.2 MB.

TABLE S2, XLSX file, 0.1 MB.

TABLE S3, XLSX file, 0.02 MB.

TABLE S4, XLSX file, 0.01 MB.

ACKNOWLEDGMENTS

The authors are grateful to Élise Lacroix from the greenhouse platform at UCBL for her precious help in the maintenance of plants. The first author also thanks the EuroXanth COST Action CA16107 and the FNX network for the scientific meeting opportunities they provided. This work benefited from the facilities and expertise of the high-throughput sequencing core facility of I2BC (Centre de Recherche de Gif [<http://www.i2bc.paris-saclay.fr/>]). We also thank Annie Buchwalter for English proofreading and corrections.

The LABGeM (CEA/Genoscope and CNRS UMR8030) and the France Génomique and French Bioinformatics Institute national infrastructures (funded as part of Investissement d’Avenir program managed by Agence Nationale pour la Recherche, contracts ANR-10-INBS-09 and ANR-11-INBS-0013) are acknowledged for support within the MicroScope annotation platform.

REFERENCES

- Kraepiel Y, Barny M. 2016. Gram-negative phytopathogenic bacteria, all hemibiotrophs after all? *Mol Plant Pathol* 17:313–316. <https://doi.org/10.1111/mpp.12345>.
- Pierella Karlusich JJ, Zurbruggen MD, Shahinnia F, Sonnewald S, Sonnewald U, Hosseini SA, Hajirezaei M-R, Carrillo N. 2017. chloroplast redox status modulates genome-wide plant responses during the non-host interaction of tobacco with the hemibiotrophic bacterium *Xanthomonas campestris* pv. *vesicatoria*. *Front Plant Sci* 8:1158. <https://doi.org/10.3389/fpls.2017.01158>.
- Islam MT, Al Mamun M, Lee B-R, Van Hien L, Jung W-J, Bae D-W, Kim T-H. 2021. Role of salicylic acid signaling in the biotrophy-necrotrophy transition of *Xanthomonas campestris* pv. *campestris* infection in *Brassica napus*. *Physiol Mol Plant Pathol* 113:101578. <https://doi.org/10.1016/j.pmp.2020.101578>.
- Luneau JS, Cerutti A, Roux B, Carrère S, Jardinaud M-F, Gaillac A, Gris C, Lauber E, Berthomé R, Arlat M, Boulanger A, Noël LD. 2022. *Xanthomonas* transcriptome inside cauliflower hydathodes reveals bacterial virulence strategies and physiological adaptations at early infection stages. *Mol Plant Pathol* 23:159–174. <https://doi.org/10.1111/mpp.13117>.
- An S-Q, Potnis N, Dow M, Vorhölter F-J, He Y-Q, Becker A, Teper D, Li Y, Wang N, Bleris L, Tang J-L. 2020. Mechanistic insights into host adaptation, virulence and epidemiology of the phytopathogen *Xanthomonas*. *FEMS Microbiol Rev* 44:1–32. <https://doi.org/10.1093/femsre/fuz024>.

6. Vorholt JA. 2012. Microbial life in the phyllosphere. *Nat Rev Microbiol* 10: 828–840. <https://doi.org/10.1038/nrmicro2910>.
7. Darsonval A, Darrasse A, Durand K, Bureau C, Cesbron S, Jacques M-A. 2009. Adhesion and fitness in the bean phyllosphere and transmission to seed of *Xanthomonas fuscans* subsp. *fuscans*. *Mol Plant Microbe Interact* 22:747–757. <https://doi.org/10.1094/MPMI-22-6-0747>.
8. Barcarolo MV, Gottig N, Ottado J, Garavaglia BS. 2020. Participation of two general stress response proteins from *Xanthomonas citri* subsp. *citri* in environmental stress adaptation and virulence. *FEMS Microbiol Ecol* 96:faa138. <https://doi.org/10.1093/femsec/faa138>.
9. Déjean G, Blanvillain-Baufumé S, Boulanger A, Darrasse A, de Bernonville TD, Girard A-L, Carrère S, Jamet S, Zischek C, Lautier M, Solé M, Büttner D, Jacques M-A, Lauber E, Arlat M. 2013. The xylan utilization system of the plant pathogen *Xanthomonas campestris* pv. *campestris* controls epiphytic life and reveals common features with oligotrophic bacteria and animal gut symbionts. *New Phytol* 198:899–915. <https://doi.org/10.1111/nph.12187>.
10. Blanvillain S, Meyer D, Boulanger A, Lautier M, Guynet C, Denancé N, Vasse J, Lauber E, Arlat M. 2007. Plant carbohydrate scavenging through TonB-dependent receptors: a feature shared by phytopathogenic and aquatic bacteria. *PLoS One* 2:e224. <https://doi.org/10.1371/journal.pone.0000224>.
11. Boulanger A, Zischek C, Lautier M, Jamet S, Rival P, Carrere S, Arlat M, Lauber E. 2014. The plant pathogen *Xanthomonas campestris* pv. *campestris* exploits N-acetylglucosamine during infection. *mBio* 5:e01527-14.
12. Rigano LA, Siciliano F, Enrique R, Sendín L, Filippone P, Torres PS, Qüesta J, Dow JM, Castagnaro AP, Vojnov AA, Marano MR. 2007. Biofilm formation, epiphytic fitness, and canker development in *Xanthomonas axonopodis* pv. *citri*. *Mol Plant Microbe Interact* 20:1222–1230. <https://doi.org/10.1094/MPMI-20-10-1222>.
13. Boller T, Felix G. 2009. A renaissance of elicitors: perception of microbe-associated molecular patterns and danger signals by pattern-recognition receptors. *Annu Rev Plant Biol* 60:379–406. <https://doi.org/10.1146/annurev.arplant.57.032905.105346>.
14. Aslam SN, Newman M-A, Erbs G, Morrissey KL, Chinchilla D, Boller T, Jensen TT, De Castro C, Ierano T, Molinaro A, Jackson RW, Knight MR, Cooper RM. 2008. Bacterial polysaccharides suppress induced innate immunity by calcium chelation. *Curr Biol* 18:1078–1083. <https://doi.org/10.1016/j.cub.2008.06.061>.
15. Silipo A, Erbs G, Shinya T, Dow JM, Parrilli M, Lanzetta R, Shibuya N, Newman M-A, Molinaro A. 2010. Glyco-conjugates as elicitors or suppressors of plant innate immunity. *Glycobiology* 20:406–419. <https://doi.org/10.1093/glycob/cwp201>.
16. Fatima U, Senthil-Kumar M. 2015. Plant and pathogen nutrient acquisition strategies. *Front Plant Sci* 6:750. <https://doi.org/10.3389/fpls.2015.00750>.
17. Timilsina S, Potnis N, Newberry EA, Liyanapathirana P, Iruegas-Bocardo F, White FF, Goss EM, Jones JB. 2020. *Xanthomonas* diversity, virulence and plant–pathogen interactions. *Nat Rev Microbiol* 18:415–427. <https://doi.org/10.1038/s41579-020-0361-8>.
18. Morinière L, Bulet A, Rosenthal ER, Nesme X, Portier P, Bull CT, Lavire C, Fischer-Le Saux M, Bertolla F. 2020. Clarifying the taxonomy of the causal agent of bacterial leaf spot of lettuce through a polyphasic approach reveals that *Xanthomonas cynarae* Trébaol et al. 2000 emend. Timilsina et al. 2019 is a later heterotypic synonym of *Xanthomonas hortorum* Vauterin et al. 1995. *Syst Appl Microbiol* 43:126087. <https://doi.org/10.1016/j.syapm.2020.126087>.
19. Bull CT, Koike ST. 2005. Evaluating the efficacy of commercial products for management of bacterial leaf spot on lettuce. *Plant Health Prog* <https://doi.org/10.1094/PHP-2005-1121-01-RS>.
20. Ozyilmaz U, Benioglu K. 2018. Bacterial leaf spot of lettuce caused by *Xanthomonas hortorum* pv. *vitians* in the Aegean Region of Turkey. *Australas Plant Dis Notes* 13:37. <https://doi.org/10.1007/s13314-018-0325-2>.
21. Koike ST, Gilbertson RL. 2017. Detection of *Xanthomonas campestris* pv. *vitians* in lettuce seeds, p 173–178. In Fatmi M, Walcott RR, Schaad NW (ed), *Detection of plant-pathogenic bacteria in seed and other planting material*, 2nd ed. APS Press, St Paul, MN.
22. Sandoya GV, Maisonneuve B, Truco MJ, Bull CT, Simko I, Trent M, Hayes RJ, Michelmore RW. 2019. Genetic analysis of resistance to bacterial leaf spot in the heirloom lettuce cultivar Reine des Glaces. *Mol Breed* 39:160. <https://doi.org/10.1007/s11032-019-1072-6>.
23. Myung I-S, Moon SY, Jeong IH, Lee SW, Lee YH, Shim HS. 2010. Bacterial leaf spot of iceberg lettuce caused by *Xanthomonas campestris* pv. *vitians* type B, a new disease in South Korea. *Plant Dis* 94:790–790. <https://doi.org/10.1094/PDIS-94-6-0790B>.
24. Dia NC, Morinière L, Cottyn B, Bernal E, Jacobs JM, Koebnik R, Osdaghi E, Potnis N, Pothier JF. 2022. *Xanthomonas hortorum*—beyond gardens: current taxonomy, genomics, and virulence repertoires. *Mol Plant Pathol* <https://doi.org/10.1111/mpp.13185>.
25. Morinière L, Lecomte S, Gueguen E, Bertolla F. 2021. *In vitro* exploration of the *Xanthomonas hortorum* pv. *vitians* genome using transposon insertion sequencing and comparative genomics to discriminate between core and contextual essential genes. *Microb Genom* 7:e000546. <https://doi.org/10.1099/mgen.0.000546>.
26. van Opijnen T, Bodi KL, Camilli A. 2009. Tn-seq; high-throughput parallel sequencing for fitness and genetic interaction studies in microorganisms. *Nat Methods* 6:767–772. <https://doi.org/10.1038/nmeth.1377>.
27. Fabian BK, Tetu SG, Paulsen IT. 2020. Application of transposon insertion sequencing to agricultural science. *Front Plant Sci* 11:291. <https://doi.org/10.3389/fpls.2020.00291>.
28. Duong DA, Jensen RV, Stevens AM. 2018. Discovery of *Pantoea stewartii* ssp. *stewartii* genes important for survival in corn xylem through a Tn-Seq analysis. *Mol Plant Pathol* 19:1929–1941. <https://doi.org/10.1111/mpp.12669>.
29. Royet K, Parisot N, Rodrigue A, Gueguen E, Condemine G. 2019. Identification by Tn-seq of *Dickeya dadantii* genes required for survival in chicory plants. *Mol Plant Pathol* 20:287–306. <https://doi.org/10.1111/mpp.12754>.
30. Helmann TC, Deutschbauer AM, Lindow SE. 2019. Genome-wide identification of *Pseudomonas syringae* genes required for fitness during colonization of the leaf surface and apoplast. *Proc Natl Acad Sci U S A* 116: 18900–18910. <https://doi.org/10.1073/pnas.1908858116>.
31. Helmann TC, Deutschbauer AM, Lindow SE. 2020. Distinctiveness of genes contributing to growth of *Pseudomonas syringae* in diverse host plant species. *PLoS One* 15:e0239998. <https://doi.org/10.1371/journal.pone.0239998>.
32. Su Y, Xu Y, Liang H, Yuan G, Wu X, Zheng D. 2021. Genome-wide identification of *Ralstonia solanacearum* genes required for survival in tomato plants. *mSystems* 6:e00838-21. <https://doi.org/10.1128/mSystems.00838-21>.
33. Torres M, Jiquel A, Jeanne E, Naquin D, Dessaux Y, Faure D. 2022. *Agrobacterium tumefaciens* fitness genes involved in the colonization of plant tumors and roots. *New Phytol* 233:905–918. <https://doi.org/10.1111/nph.17810>.
34. Chao MC, Abel S, Davis BM, Waldor MK. 2016. The design and analysis of transposon-insertion sequencing experiments. *Nat Rev Microbiol* 14: 119–128. <https://doi.org/10.1038/nrmicro.2015.7>.
35. Abel S, Abel Zur Wiesch P, Chang H-H, Davis BM, Lipsitch M, Waldor MK. 2015. Sequence tag-based analysis of microbial population dynamics. *Nat Methods* 12:223–226. <https://doi.org/10.1038/nmeth.3253>.
36. Mahmutovic A, Abel Zur Wiesch P, Abel S. 2020. Selection or drift: the population biology underlying transposon insertion sequencing experiments. *Comput Struct Biotechnol J* 18:791–804. <https://doi.org/10.1016/j.csbj.2020.03.021>.
37. van Opijnen T, Camilli A. 2013. Transposon insertion sequencing: a new tool for systems-level analysis of microorganisms. *Nat Rev Microbiol* 11: 435–442. <https://doi.org/10.1038/nrmicro3033>.
38. Liu Z, Beskronnaya P, Melnyk RA, Hossain SS, Khorasani S, O’Sullivan LR, Wiesmann CL, Bush J, Richard JD, Haney CH. 2018. A genome-wide screen identifies genes in rhizosphere-associated *Pseudomonas* required to evade plant defenses. *mBio* 9:e00433-18. <https://doi.org/10.1128/mBio.00433-18>.
39. Gene Ontology Consortium. 2021. The Gene Ontology resource: enriching a GOld mine. *Nucleic Acids Res* 49:D325–D334. <https://doi.org/10.1093/nar/gkaa1113>.
40. Kanehisa M, Sato Y, Morishima K. 2016. BlastKOALA and GhostKOALA: KEGG tools for functional characterization of genome and metagenome sequences. *J Mol Biol* 428:726–731. <https://doi.org/10.1016/j.jmb.2015.11.006>.
41. Qian W, Jia Y, Ren S-X, He Y-Q, Feng J-X, Lu L-F, Sun Q, Ying G, Tang D-J, Tang H, Wu W, Hao P, Wang L, Jiang B-L, Zeng S, Gu W-Y, Lu G, Rong L, Tian Y, Yao Z, Fu G, Chen B, Fang R, Qiang B, Chen Z, Zhao G-P, Tang J-L, He C. 2005. Comparative and functional genomic analyses of the pathogenicity of phytopathogen *Xanthomonas campestris* pv. *campestris*. *Genome Res* 15:757–767. <https://doi.org/10.1101/gr.3378705>.
42. Wang JC, So BH, Kim JH, Park YJ, Lee BM, Kang HW. 2008. Genome-wide identification of pathogenicity genes in *Xanthomonas oryzae* pv. *oryzae* by transposon mutagenesis. *Plant Pathol* 57:1136–1145. <https://doi.org/10.1111/j.1365-3059.2008.01884.x>.
43. Song X, Guo J, Ma W, Ji Z, Zou L, Chen G, Zou H. 2015. Identification of seven novel virulence genes from *Xanthomonas citri* subsp. *citri* by Tn5-based random mutagenesis. *J Microbiol* 53:330–336. <https://doi.org/10.1007/s12275-015-4589-3>.

44. Zou H-S, Yuan L, Guo W, Li Y-R, Che Y-Z, Zou L-F, Chen G-Y. 2011. Construction of a Tn5-tagged mutant library of *Xanthomonas oryzae* pv. *oryzicola* as an invaluable resource for functional genomics. *Curr Microbiol* 62:908–916. <https://doi.org/10.1007/s00284-010-9804-1>.
45. Matilla MA, Krell T. 2018. The effect of bacterial chemotaxis on host infection and pathogenicity. *FEMS Microbiol Rev* 42:fux052. <https://doi.org/10.1093/femsre/fux052>.
46. Darrasse A, Carrère S, Barbe V, Boureau T, Arrieta-Ortiz ML, Bonneau S, Briand M, Brin C, Cociancich S, Durand K, Fouteau S, Gagnevin L, Guérin F, Guy E, Indiana A, Koebnik R, Lauber E, Munoz A, Noël LD, Pieretti I, Poussier S, Pruvost O, Robène-Soustrade I, Rott P, Royer M, Serres-Gardi L, Szurek B, van Sluys M-A, Verdier V, Vernière C, Arlat M, Manceau C, Jacques M-A. 2013. Genome sequence of *Xanthomonas fuscans* subsp. *fuscans* strain 4834-R reveals that flagellar motility is not a general feature of xanthomonads. *BMC Genomics* 14:761. <https://doi.org/10.1186/1471-2164-14-761>.
47. Liao Z-X, Ni Z, Wei X-L, Chen L, Li J-Y, Yu Y-H, Jiang W, Jiang B-L, He Y-Q, Huang S. 2019. Dual RNA-seq of *Xanthomonas oryzae* pv. *oryzicola* infecting rice reveals novel insights into bacterial-plant interaction. *PLoS One* 14:e0215039. <https://doi.org/10.1371/journal.pone.0215039>.
48. Nobori T, Velásquez AC, Wu J, Kvitko BH, Kremer JM, Wang Y, He SY, Tsuda K. 2018. Transcriptome landscape of a bacterial pathogen under plant immunity. *Proc Natl Acad Sci U S A* 115:E3055–E3064. <https://doi.org/10.1073/pnas.1800529115>.
49. Rico A, Preston GM. 2008. *Pseudomonas syringae* pv. *tomato* DC3000 uses constitutive and apoplast-induced nutrient assimilation pathways to catabolize nutrients that are abundant in the tomato apoplast. *Mol Plant Microbe Interact* 21:269–282. <https://doi.org/10.1094/MPMI-21-2-0269>.
50. Lohaus G, Winter H, Riens B, Heldt HW. 1995. Further studies of the phloem loading process in leaves of barley and spinach. The comparison of metabolite concentrations in the apoplastic compartment with those in the cytosolic compartment and in the sieve tubes. *Bot Acta* 108:270–275. <https://doi.org/10.1111/j.1438-8677.1995.tb00860.x>.
51. O'Leary BM, Neale HC, Geilfus C-M, Jackson RW, Arnold DL, Preston GM. 2016. Early changes in apoplast composition associated with defence and disease in interactions between *Phaseolus vulgaris* and the halo blight pathogen *Pseudomonas syringae* pv. *phaseolicola*. *Plant Cell Environ* 39:2172–2184. <https://doi.org/10.1111/pce.12770>.
52. Joosten MHAJ, Hendrickx LJM, Wit PJGM. 1990. Carbohydrate composition of apoplastic fluids isolated from tomato leaves inoculated with virulent or avirulent races of *Cladosporium fulvum* (syn. *Fulvia fulva*). *Neth J Plant Pathol* 96:103–112. <https://doi.org/10.1007/BF02005134>.
53. Szczesny R, Jordan M, Schramm C, Schulz S, Cogege V, Bonas U, Büttner D. 2010. Functional characterization of the Xcs and Xps type II secretion systems from the plant pathogenic bacterium *Xanthomonas campestris* pv. *vesicatoria*. *New Phytol* 187:983–1002. <https://doi.org/10.1111/j.1469-8137.2010.03312.x>.
54. Vandroemme J, Cottyn B, Baeyen S, De Vos P, Maes M. 2013. Draft genome sequence of *Xanthomonas fragariae* reveals reductive evolution and distinct virulence-related gene content. *BMC Genomics* 14:829. <https://doi.org/10.1186/1471-2164-14-829>.
55. Kim H-S, Park H-J, Heu S, Jung J. 2004. Molecular and functional characterization of a unique sucrose hydrolase from *Xanthomonas axonopodis* pv. *glycines*. *J Bacteriol* 186:411–418. <https://doi.org/10.1128/JB.186.2.411-418.2004>.
56. Watt TF, Vucur M, Baumgarth B, Watt SA, Niehaus K. 2009. Low molecular weight plant extract induces metabolic changes and the secretion of extracellular enzymes, but has a negative effect on the expression of the type-III secretion system in *Xanthomonas campestris* pv. *campestris*. *J Biotechnol* 140:59–67. <https://doi.org/10.1016/j.jbiotec.2008.12.003>.
57. Zhang C, Lv M, Yin W, Dong T, Chang C, Miao Y, Jia Y, Deng Y. 2019. *Xanthomonas campestris* promotes diffusible signal factor biosynthesis and pathogenicity by utilizing glucose and sucrose from host plants. *Mol Plant Microbe Interact* 32:157–166. <https://doi.org/10.1094/MPMI-07-18-0187-R>.
58. He Y-W, Zhang L-H. 2008. Quorum sensing and virulence regulation in *Xanthomonas campestris*. *FEMS Microbiol Rev* 32:842–857. <https://doi.org/10.1111/j.1574-6976.2008.00120.x>.
59. Chow V, Shanharaj D, Guo Y, Nong G, Minsavage GV, Jones JB, Preston JF. 2015. Xylan utilization regulon in *Xanthomonas citri* pv. *citri* strain 306: gene expression and utilization of oligoxylosides. *Appl Environ Microbiol* 81:2163–2172. <https://doi.org/10.1128/AEM.03091-14>.
60. Santos CR, Hoffmam ZB, de Matos Martins VP, Zanphorlin LM, de Paula Assis LH, Honorato RV, Lopes de Oliveira PS, Ruller R, Murakami MT. 2014. Molecular mechanisms associated with xylan degradation by *Xanthomonas* plant pathogens. *J Biol Chem* 289:32186–32200. <https://doi.org/10.1074/jbc.M114.605105>.
61. Pandey SS, Patnana PK, Rai R, Chatterjee S. 2017. Xanthoferrin, the α -hydroxycarboxylate-type siderophore of *Xanthomonas campestris* pv. *campestris*, is required for optimum virulence and growth inside cabbage. *Mol Plant Pathol* 18:949–962. <https://doi.org/10.1111/mpp.12451>.
62. Guerra GS, Balan A. 2020. Genetic and structural determinants on iron assimilation pathways in the plant pathogen *Xanthomonas citri* subsp. *citri* and *Xanthomonas* sp. *Braz J Microbiol* 51:1219–1231. <https://doi.org/10.1007/s42770-019-00207-x>.
63. Liu Y, Kong D, Wu H-L, Ling H-Q. 2021. Iron in plant-pathogen interactions. *J Exp Bot* 72:2114–2124. <https://doi.org/10.1093/jxb/eraa516>.
64. Távora FTPK, Santos C, Maximiano MR, Murad AM, Oliveira-Neto OB, Megias E, Junior FBR, Franco OL, Mehta A. 2019. Pan proteome of *Xanthomonas campestris* pv. *campestris* isolates contrasting in virulence. *Proteomics* 19:1900082. <https://doi.org/10.1002/pmic.201900082>.
65. Cain AK, Barquist L, Goodman AL, Paulsen IT, Parkhill J, van Opijnen T. 2020. A decade of advances in transposon-insertion sequencing. *Nat Rev Genet* 21:526–540. <https://doi.org/10.1038/s41576-020-0244-x>.
66. Vorhölter F-J, Schneiker S, Goesmann A, Krause L, Bekel T, Kaiser O, Linke B, Patschkowski T, Rückert C, Schmid J, Sidhu VK, Sieber V, Tauch A, Watt SA, Weisshaar B, Becker A, Niehaus K, Pühler A. 2008. The genome of *Xanthomonas campestris* pv. *campestris* B100 and its use for the reconstruction of metabolic pathways involved in xanthan biosynthesis. *J Biotechnol* 134:33–45. <https://doi.org/10.1016/j.jbiotec.2007.12.013>.
67. Galván EM, Ielmini MV, Patel YN, Bianco MI, Franceschini EA, Schneider JC, Ielpi L. 2013. Xanthan chain length is modulated by increasing the availability of the polysaccharide copolymerase protein GumC and the outer membrane polysaccharide export protein GumB. *Glycobiology* 23:259–272. <https://doi.org/10.1093/glycob/cws146>.
68. Kim S-Y, Kim J-G, Lee B-M, Cho J-Y. 2009. Mutational analysis of the *gum* gene cluster required for xanthan biosynthesis in *Xanthomonas oryzae* pv. *oryzae*. *Biotechnol Lett* 31:265–270. <https://doi.org/10.1007/s10529-008-9858-3>.
69. Klein G, Kobylak N, Lindner B, Stupak A, Raina S. 2014. Assembly of lipopolysaccharide in *Escherichia coli* requires the essential LapB heat shock protein. *J Biol Chem* 289:14829–14853. <https://doi.org/10.1074/jbc.M113.539494>.
70. Petrocelli S, Tondo ML, Daurelio LD, Orellano EG. 2012. Modifications of *Xanthomonas axonopodis* pv. *citri* lipopolysaccharide affect the basal response and the virulence process during citrus canker. *PLoS One* 7:e40051. <https://doi.org/10.1371/journal.pone.0040051>.
71. Guo Y, Sagaram US, Kim J, Wang N. 2010. Requirement of the *galU* gene for polysaccharide production by and pathogenicity and growth in planta of *Xanthomonas citri* subsp. *citri*. *Appl Environ Microbiol* 76:2234–2242. <https://doi.org/10.1128/AEM.02897-09>.
72. Vorhölter F-J, Niehaus K, Pühler A. 2001. Lipopolysaccharide biosynthesis in *Xanthomonas campestris* pv. *campestris*: a cluster of 15 genes is involved in the biosynthesis of the LPS O-antigen and the LPS core. *Mol Genet Genomics* 266:79–95. <https://doi.org/10.1007/s004380100521>.
73. Köpflin R, Wang G, Hötte B, Priefer UB, Pühler A. 1993. A 3.9-kb DNA region of *Xanthomonas campestris* pv. *campestris* that is necessary for lipopolysaccharide production encodes a set of enzymes involved in the synthesis of dTDP-rhamnose. *J Bacteriol* 175:7786–7792. <https://doi.org/10.1128/jb.175.24.7786-7792.1993>.
74. Molinaro A, Castro CD, Lanzetta R, Parrilli M, Petersen BO, Broberg A, Duus JØ. 2002. NMR and MS evidences for a random assembled O-specific chain structure in the LPS of the bacterium *Xanthomonas campestris* pv. *vitians*. *Eur J Biochem* 269:4185–4193. <https://doi.org/10.1046/j.1432-1033.2002.03138.x>.
75. Steffens T, Vorhölter F-J, Giampà M, Hublik G, Pühler A, Niehaus K. 2016. The influence of a modified lipopolysaccharide O-antigen on the biosynthesis of xanthan in *Xanthomonas campestris* pv. *campestris* B100. *BMC Microbiol* 16:93. <https://doi.org/10.1186/s12866-016-0710-y>.
76. Rætz CRH, Whitfield C. 2002. Lipopolysaccharide endotoxins. *Annu Rev Biochem* 71:635–700. <https://doi.org/10.1146/annurev.biochem.71.110601.135414>.
77. Matsuura M. 2013. Structural modifications of bacterial lipopolysaccharide that facilitate Gram-negative bacteria evasion of host innate immunity. *Front Immunol* 4:109. <https://doi.org/10.3389/fimmu.2013.00109>.

78. Newman M-A, Dow JM, Daniels MJ. 2001. Bacterial lipopolysaccharides and plant-pathogen interactions. *Eur J Plant Pathol* 107:95–102. <https://doi.org/10.1023/A:1008738817551>.
79. Rapicavoli JN, Blanco-Ulate B, Muszyński A, Figueroa-Balderas R, Morales-Cruz A, Azadi P, Dobruchowska JM, Castro C, Cantu D, Roper MC. 2018. Lipopolysaccharide O-antigen delays plant innate immune recognition of *Xylella fastidiosa*. *Nat Commun* 9:390. <https://doi.org/10.1038/s41467-018-02861-5>.
80. Lushchak VI. 2001. Oxidative stress and mechanisms of protection against it in bacteria. *Biochem Mosc* 66:476–489. <https://doi.org/10.1023/A:1010294415625>.
81. Fones H, Preston GM. 2012. Reactive oxygen and oxidative stress tolerance in plant pathogenic *Pseudomonas*. *FEMS Microbiol Lett* 327:1–8. <https://doi.org/10.1111/j.1574-6968.2011.02449.x>.
82. Santos R, Franza T, Laporte M-L, Sauvage C, Touati D, Expert D. 2001. Essential role of superoxide dismutase on the pathogenicity of *Erwinia chrysanthemi* strain 3937. *Mol Plant Microbe Interact* 14:758–767. <https://doi.org/10.1094/MPMI.2001.14.6.758>.
83. Hugouvieux V, Barber CE, Daniels MJ. 1998. Entry of *Xanthomonas campestris* pv. *campestris* into hydathodes of *Arabidopsis thaliana* leaves: a system for studying early infection events in bacterial pathogenesis. *Mol Plant Microbe Interact* 11:537–543. <https://doi.org/10.1094/MPMI.1998.11.6.537>.
84. Smith SG, Wilson TJ, Dow JM, Daniels MJ. 1996. A gene for superoxide dismutase from *Xanthomonas campestris* pv. *campestris* and its expression during bacterial-plant interactions. *Mol Plant Microbe Interact* 9:584–593. <https://doi.org/10.1094/mpmi-9-0584>.
85. Lin C-N, Syu W-J, Sun W-SW, Chen J-W, Chen T-H, Don M-J, Wang S-H. 2010. A role of *ygfZ* in the *Escherichia coli* response to plumbagin challenge. *J Biomed Sci* 17:84. <https://doi.org/10.1186/1423-0127-17-84>.
86. Figaj D, Ambroziak P, Przepiora T, Skorko-Glonek J. 2019. The role of proteases in the virulence of plant pathogenic bacteria. *Int J Mol Sci* 20:672. <https://doi.org/10.3390/ijms20030672>.
87. Li C-E, Liao C-T, Lo H-H, Hsiao Y-M. 2020. Functional characterization and transcriptional analysis of *clpP* of *Xanthomonas campestris* pv. *campestris*. *Curr Microbiol* 77:2876–2885. <https://doi.org/10.1007/s00284-020-02093-1>.
88. Lo H-H, Liao C-T, Li C-E, Chiang Y-C, Hsiao Y-M. 2020. The *clpX* gene plays an important role in bacterial attachment, stress tolerance, and virulence in *Xanthomonas campestris* pv. *campestris*. *Arch Microbiol* 202:597–607. <https://doi.org/10.1007/s00203-019-01772-3>.
89. Bove P, Capozzi V, Garofalo C, Rieu A, Spano G, Fiocco D. 2012. Inactivation of the *ftsH* gene of *Lactobacillus plantarum* WCF51: effects on growth, stress tolerance, cell surface properties and biofilm formation. *Microbiol Res* 167:187–193. <https://doi.org/10.1016/j.jmicsres.2011.07.001>.
90. Matos RG, Bária C, Moreira RN, Barahona S, Domingues S, Arraiano CM. 2014. The importance of proteins of the RNase II/RNB-family in pathogenic bacteria. *Front Cell Infect Microbiol* 4:68. <https://doi.org/10.3389/fcimb.2014.00068>.
91. Facincani AP, Moreira LM, Soares MR, Ferreira CB, Ferreira RM, Ferro MIT, Ferro JA, Gozzo FC, de Oliveira JCF. 2014. Comparative proteomic analysis reveals that T3SS, Tfp, and xanthan gum are key factors in initial stages of *Citrus sinensis* infection by *Xanthomonas citri* subsp. *citri*. *Funct Integr Genomics* 14:205–217. <https://doi.org/10.1007/s10142-013-0340-5>.
92. Imlay JA, Linn S. 1987. Mutagenesis and stress responses induced in *Escherichia coli* by hydrogen peroxide. *J Bacteriol* 169:2967–2976. <https://doi.org/10.1128/jb.169.7.2967-2976.1987>.
93. Stohl EA, Seifert HS. 2006. *Neisseria gonorrhoeae* DNA recombination and repair enzymes protect against oxidative damage caused by hydrogen peroxide. *J Bacteriol* 188:7645–7651. <https://doi.org/10.1128/JB.00801-06>.
94. Cano DA, Pucciarelli MG, García-del Portillo F, Casadesús J. 2002. Role of the RecBCD recombination pathway in *Salmonella* virulence. *J Bacteriol* 184:592–595. <https://doi.org/10.1128/JB.184.2.592-595.2002>.
95. Kuzminov A, Stahl FW. 1999. Double-strand end repair via the RecBC pathway in *Escherichia coli* primes DNA replication. *Genes Dev* 13:345–356. <https://doi.org/10.1101/gad.13.3.345>.
96. Mongkolsuk S, Rabibhadana S, Sukchavalit R, Vaughn G. 1998. Construction and physiological analysis of a *Xanthomonas oryzae* pv. *oryzae* *recA* mutant. *FEMS Microbiol Lett* 169:269–275. <https://doi.org/10.1111/j.1574-6968.1998.tb13328.x>.
97. Aguirre-Ramírez M, Medina G, González-Valdez A, Grosso-Becerra V, Soberón-Chávez G. 2012. The *Pseudomonas aeruginosa* *rmlBDAC* operon, encoding dTDP-l-rhamnose biosynthetic enzymes, is regulated by the quorum-sensing transcriptional regulator RhIR and the alternative sigma factor σ^S . *Microbiology (Reading)* 158:908–916. <https://doi.org/10.1099/mic.0.054726-0>.
98. Bronstein PA, Marrichi M, Cartinhour S, Schneider DJ, DeLisa MP. 2005. Identification of a twin-arginine translocation system in *Pseudomonas syringae* pv. *tomato* DC3000 and its contribution to pathogenicity and fitness. *J Bacteriol* 187:8450–8461. <https://doi.org/10.1128/JB.187.24.8450-8461.2005>.
99. Genin S, Denny TP. 2012. Pathogenomics of the *Ralstonia solanacearum* species complex. *Annu Rev Phytopathol* 50:67–89. <https://doi.org/10.1146/annurev-phyto-081211-173000>.
100. Ranjan M, Khokhani D, Nayaka S, Srivastava S, Keyser ZP, Ranjan A. 2021. Genomic diversity and organization of complex polysaccharide biosynthesis clusters in the genus *Dickeya*. *PLoS One* 16:e0245727. <https://doi.org/10.1371/journal.pone.0245727>.
101. Jayaraman J, Jones WT, Harvey D, Hemara LM, McCann HC, Yoon M, Warring SL, Fineran PC, Mesarich CH, Templeton MD. 2020. Variation at the common polysaccharide antigen locus drives lipopolysaccharide diversity within the *Pseudomonas syringae* species complex. *Environ Microbiol* 22:5356–5372. <https://doi.org/10.1111/1462-2920.15250>.
102. Georgoulis SJ, Shalvarjian KE, Helmann TC, Hamilton CD, Carlson HK, Deutschbauer AM, Lowe-Power TM. 2021. Genome-wide identification of tomato xylem sap fitness factors for three plant-pathogenic *Ralstonia* species. *mSystems* 6:e01229-21. <https://doi.org/10.1128/mSystems.01229-21>.
103. Martin M. 2011. Cutadapt removes adapter sequences from high-throughput sequencing reads. *EMBnetj* 17:10–12. <https://doi.org/10.14806/ej.17.1.200>.
104. DeJesus MA, Ambadipudi C, Baker R, Sasseti C, Ioerger TR. 2015. TRANSIT—a software tool for Himar1 TnSeq analysis. *PLoS Comput Biol* 11:e1004401. <https://doi.org/10.1371/journal.pcbi.1004401>.
105. DeJesus MA, Ioerger TR. 2016. Normalization of transposon-mutant library sequencing datasets to improve identification of conditionally essential genes. *J Bioinform Comput Biol* 14:1642004. <https://doi.org/10.1142/S021972001642004X>.
106. Benjamini Y, Yekutieli D. 2005. False discovery rate—adjusted multiple confidence intervals for selected parameters. *J Am Stat Assoc* 100:71–81. <https://doi.org/10.1198/01621450400001907>.
107. Vallenet D, Calteau A, Dubois M, Amours P, Bazin A, Beuvin M, Burlot L, Bussell X, Fouteau S, Gautreau G, Lajus A, Langlois J, Planel R, Roche D, Rollin J, Rouy Z, Sabatet V, Médigue C. 2020. MicroScope: an integrated platform for the annotation and exploration of microbial gene functions through genomic, pangenomic and metabolic comparative analysis. *Nucleic Acids Res* 48:D579–D589. <https://doi.org/10.1093/nar/gkz926>.
108. Yu Y, Ouyang Y, Yao W. 2018. shinyCircos: an R/Shiny application for interactive creation of Circos plot. *Bioinformatics* 34:1229–1231. <https://doi.org/10.1093/bioinformatics/btx763>.
109. Leimbach A. 2016. bac-genomics-scripts: bovine E. coli mastitis comparative genomics edition. Zenodo <https://doi.org/10.5281/zenodo.215824>. Accessed 16 March 2021.
110. Huerta-Cepas J, Forslund K, Coelho LP, Szklarczyk D, Jensen LJ, von Mering C, Bork P. 2017. Fast genome-wide functional annotation through orthology assignment by eggNOG-Map. *Mol Biol Evol* 34:2115–2122. <https://doi.org/10.1093/molbev/msx148>.
111. Huerta-Cepas J, Szklarczyk D, Heller D, Hernández-Plaza A, Forslund SK, Cook H, Mende DR, Letunic I, Rattei T, Jensen LJ, von Mering C, Bork P. 2019. eggNOG 5.0: a hierarchical, functionally and phylogenetically annotated orthology resource based on 5090 organisms and 2502 viruses. *Nucleic Acids Res* 47:D309–D314. <https://doi.org/10.1093/nar/gky1085>.
112. Jones P, Binns D, Chang H-Y, Fraser M, Li W, McAnulla C, McWilliam H, Maslen J, Mitchell A, Nuka G, Pesseat S, Quinn AF, Sangrador-Vegas A, Scheremetjew M, Yong S-Y, Lopez R, Hunter S. 2014. InterProScan 5: genome-scale protein function classification. *Bioinformatics* 30:1236–1240. <https://doi.org/10.1093/bioinformatics/btu031>.
113. Rasche H, Grüning B, Dunn N, Bretraudeau A. 2018. GGA: Galaxy for genome annotation, teaching, and genomic databases. *F1000Res* 7:f1000research. <https://doi.org/10.7490/f1000research.1116181.1>.
114. Grossmann S, Bauer S, Robinson PM, Vingron M. 2007. Improved detection of overrepresentation of Gene-Ontology annotations with parent child analysis. *Bioinformatics* 23:3024–3031. <https://doi.org/10.1093/bioinformatics/btm440>.
115. Kanehisa M, Sato Y. 2020. KEGG Mapper for inferring cellular functions from protein sequences. *Protein Sci* 29:28–35. <https://doi.org/10.1002/pro.3711>.